TECHNICAL REPORT STANDARD PAGE

1. Report No.	2. Government Accession No.	3. Recipient's Catalog No.
FHWA/LA.08/474		

4. Title and Subtitle	5. Report Date
Accelerated Loading Evaluation of Stabilized BCS Layers in Pavement Performance	March 2012
	6. Performing Organization Code LTRC Project Number: 03-2GT State Project Number: 736-99-1124

7. Author(s)	8. Performing Organization Report No.
Zhong Wu, Zhongjie "Doc" Zhang, and William M. King, Jr.	

9. Performing Organization Name and Address	10. Work Unit No.
Louisiana Transportation Research Center 4101 Gourrier Avenue Baton Rouge, LA 70808	11. Contract or Grant No. 03-2GT

12. Sponsoring Agency Name and Address	13. Type of Report and Period Covered
Louisiana Transportation Research Center 4101 Gourrier Avenue Baton Rouge, LA 70808	**Final Report (2005-2008)**
	14. Sponsoring Agency Code

15. Supplementary Notes

Conducted in Cooperation with the U.S. Department of Transportation, Federal Highway Administration

16. Abstract

BCS is short for blended calcium sulfate, a recycled fluorogypsum mixture that has been used in Louisiana as a roadway base for more than a decade. Without further chemical stabilization, the major concern of using raw BCS as a pavement structural layer is its moisture susceptibility.

In order to verify the efficiency of laboratory-derived BCS stabilization schemes and further assess related field performance and potential cost benefits, an accelerated pavement testing (APT) experiment was recently conducted at Louisiana Transportation Research Center (LTRC) using the Accelerated Loading Facility (ALF). The APT experiment included three different base test sections: the first one contained a granulated ground blast furnace slag stabilized BCS base course (called BCS/Slag), the second used a fly ash stabilized BCS base course (called BCS/Flyash), and the third had a crushed limestone base. Except for using different base materials, the three APT sections shared a common pavement structure: a 2-in. asphalt wearing course, an 8.5-in. base course, and a 12-in. lime-treated working table layer over an A-6 soil subgrade. Each section was instrumented with one multi-depth deflectometer and two pressure cells for measuring ALF moving load induced pavement responses (i.e., deflections and vertical stresses). The instrumentation data were collected at approximately every 8,500 ALF load repetitions; whereas, non-destructive deflection tests and surface distress surveys (for surface rutting and cracking) were performed at every 25,000 ALF load passes.

The accelerated loading results generally indicated that the test section with a BCS/Slag base course outperformed the other two APT sections (i.e., the BCS/Flyash and the crushed stone sections) by a large margin. This was evidenced by all measurements in surface deflection, vertical compressive stress, rutting resistance, and pavement life. Post-mortem trench results revealed that the BCS/Slag base performed just like a lean concrete layer inside the pavement without any moisture-induced damage issues. The backcalculated layer moduli of the BCS/Slag base ranged from 1,190 ksi to 2,730 ksi, much higher than that of an asphalt concrete layer. In addition, the BCS/Flyash test section performed significantly better than the crushed stone test section in terms of the load carrying capacity, rutting resistance, and pavement life. However, post-mortem trench results showed a shear failure initialized inside the BCS/Flyash base layer on a failed station of the corresponding test section. Whether or not such a shear failure is indicative of a long-term moisture-susceptibility problem for the BCS/Flyash base layer, especially under a constantly wet environment, remains a concern due to the relatively short loading period associated with any APT experiment. Based on APT results, it was estimated that structural layer coefficients for the BCS/Slag and BCS/Flyash base courses used in this APT study would be 0.34 and 0.29, respectively.

A cost-benefit analysis showed that the implementation of a slag stabilized BCS base in lieu of a crushed stone base will lead to a thinner asphalt pavement design, which can result in an initial construction cost reduction up to 16 percent without compromising future pavement performance. On the other hand, a 30-year life cycle cost analysis (LCCA) based on a typical Louisiana low volume road pavement structure indicated that using an 8.5-in. slag stabilized or 8.5-in. fly ash stabilized BCS base course, in lieu of a 8.5-in. crushed stone base, will potentially result in an LCCA cost savings up to 62 percent and 56 percent per lane mile, respectively.

Overall, it is concluded that both the slag and fly ash stabilized BCS materials evaluated in the study should be a good base material candidate for a flexible pavement design in Louisiana. However, caution should be made when using a fly ash stabilized BCS base under a constantly wet environment.

17. Key Words	18. Distribution Statement
Stabilized Base, Pavement Performance, APT, BCS, Fly ash, Slag, Stone. LCCA	**Unrestricted. This document is available through the National Technical Information Service, Springfield, VA 21161.**

19. Security Classif. (of this report)	20. Security Classif. (of this page)	21. No. of Pages	22. Price
		101	

Project Review Committee

Each research project will have an advisory committee appointed by the LTRC Director. The Project Review Committee is responsible for assisting the LTRC Administrator or Manager in the development of acceptable research problem statements, requests for proposals, review of research proposals, oversight of approved research projects, and implementation of findings.

LTRC appreciates the dedication of the following Project Review Committee Members in guiding this research study to fruition.

LTRC Administrator

Zhongjie "Doc" Zhang
Pavement and Geotechnical Research Administrator

Members

Phil Arena
Mike Boudreaux
Jeff Lambert
Masood Rasoulian
Don Weathers
Luanna Cambas
Mark Stinson
Neal West
Said Ismail
Simone Ardoin

Directorate Implementation Sponsor

Richard Savoie, P.E.
DOTD Chief Engineer

Accelerated Loading Evaluation of Stabilized BCS Layers in Pavement Performance

by

Zhong Wu, Ph.D., P.E.
Zhongjie "Doc" Zhang, Ph.D., P.E.
William M. King, Jr., P.E.

Louisiana Transportation Research Center
4101 Gourrier Avenue
Baton Rouge, LA 70808

LTRC Project No. 03-2GT
State Project No. 736-99-1124

conducted for

Louisiana Department of Transportation and Development
Louisiana Transportation Research Center

March 2012

ABSTRACT

BCS is short for blended calcium sulfate, a recycled fluorogypsum mixture that has been used in Louisiana as a roadway base for more than a decade. Without further chemical stabilization, the major concern of using raw BCS as a pavement structural layer is its moisture susceptibility.

In order to verify the efficiency of laboratory-derived BCS stabilization schemes and further assess related field performance and potential cost benefits, an accelerated pavement testing (APT) experiment was recently conducted at Louisiana Transportation Research Center (LTRC) using the Accelerated Loading Facility (ALF). The APT experiment included three different base test sections: the first one contained a granulated ground blast furnace slag stabilized BCS base course (called BCS/Slag), the second used a fly ash stabilized BCS base course (called BCS/Flyash), and the third had a crushed limestone base. Except for using different base materials, the three APT sections shared a common pavement structure: a 2-in. asphalt wearing course, an 8.5-in. base course, and a 12-in. lime-treated working table layer over an A-6 soil subgrade. Each section was instrumented with one multi-depth deflectometer and two pressure cells for measuring ALF moving load induced pavement responses (i.e., deflections and vertical stresses). The instrumentation data were collected at approximately every 8,500 ALF load repetitions; whereas, non-destructive deflection tests and surface distress surveys (for surface rutting and cracking) were performed at every 25,000 ALF load passes.

The accelerated loading results generally indicated that the test section with a BCS/Slag base course outperformed the other two APT sections (i.e., the BCS/Flyash and the crushed stone sections) by a large margin. This was evidenced by all measurements in surface deflection, vertical compressive stress, rutting resistance, and pavement life. Post-mortem trench results revealed that the BCS/Slag base performed just like a lean concrete layer inside the pavement without any moisture-induced damage issues. The backcalculated layer moduli of the BCS/Slag base ranged from 1,190 ksi to 2,730 ksi, much higher than that of an asphalt concrete layer. In addition, the BCS/Flyash test section performed significantly better than the crushed stone test section in terms of the load carrying capacity, rutting resistance, and pavement life. However, post-mortem trench results showed a shear failure initialized inside the BCS/Flyash base layer on a failed station of the corresponding test section. Whether or not such a shear failure is indicative of a long-term moisture-susceptibility problem for the BCS/Flyash base layer, especially under a constantly wet environment, remains a concern due to the relatively short loading period associated with any APT experiment. Based on

APT results, it was estimated that structural layer coefficients for the BCS/Slag and BCS/Flyash base courses used in this APT study would be 0.34 and 0.29, respectively.

A cost-benefit analysis showed that the implementation of a slag stabilized BCS base in lieu of a crushed stone base will lead to a thinner asphalt pavement design, which can result in an initial construction cost reduction up to 16 percent without compromising future pavement performance. On the other hand, a 30-year life cycle cost analysis (LCCA) based on a typical Louisiana low volume road pavement structure indicated that using an 8.5-in. slag stabilized or 8.5-in. fly ash stabilized BCS base course, in lieu of a 8.5-in. crushed stone base, will potentially result in an LCCA cost savings up to 62 percent and 56 percent per lane mile, respectively.

Overall, it is concluded that both the slag and fly ash stabilized BCS materials evaluated in the study should be a good base material candidate for a flexible pavement design in Louisiana. However, caution should be made when using a fly ash stabilized BCS base under a constantly wet environment.

ACKNOWLEDGMENTS

This study was supported by LTRC and the Louisiana Department of Transportation and Development (LADOTD). The authors would like to express thanks to all those who provided valuable help in this study.

IMPLEMENTATION STATEMENT

This experiment demonstrated in a field environment that both a 10 percent slag by volume and 15 percent fly ash by volume stabilized BCS can serve as a good pavement base course material in lieu of a typical Class-II crushed limestone base course currently used by LADOTD. In fact, the 10 percent slag stabilized BCS was observed to have a significantly better rut-resistance than the crushed limestone base course studied. No cracking was found in the slag BCS test section at the end of the current experiment. Therefore, the researchers recommend that LADOTD consider using a 10 percent slag by volume stabilized BCS in both medium and high volume roads. A 15 percent fly ash by volume stabilized BCS can also be used in lieu of a Class-II crushed limestone base due to its outstanding field rut-resistance and favorable cost savings showed in a life cycle cost analysis. The researchers also recommend that LADOTD use the slag stabilized BCS materials in perpetual flexible pavement design, where a full-depth asphalt concrete layer may be partially replaced by a slag stabilized BCS layer without compromising its long-lasting pavement performance.

TABLE OF CONTENTS

LIST OF TABLES

LIST OF FIGURES

INTRODUCTION

Using industrial or mineral waste materials in pavement engineering not only provides construction materials with possible savings over new materials, but it also reduces demands on natural construction materials. It also can protect the environment and save money through reducing the amount of waste materials requiring disposal. Due to a lack of natural resources of high-quality stone aggregates in Louisiana, LADOTD is always seeking alternative materials for replacing the crushed stone in a roadway base construction. One alternative base material is recycled fluorogypsum, an industrial by-product of hydrofluoric acid production from fluorspar (a mineral composed of calcium fluoride) and sulfuric acid. For an environmental safety purpose, recycling of fluorogypsum requires adding lime or limestone to raise its pH value. In Louisiana, a recycled fluorogypsum base is also called the BCS (blended calcium sulfate) base in roadway construction.

LADOTD began to use BCS as an alternative base material in the 1990s. According to the Louisiana Standard Specifications for Road and Bridge, the constructed BCS base is required to have the same gradation limit as a regular stone base *[1]*. Raw BCS base (i.e., without further chemical stabilization) can achieve relatively high strength and stiffness under a dry environment. However, raw BCS is associated with a moisture susceptibility problem, which can usually cause construction difficulties.

In a previously completed laboratory study (LTRC Final Report No. 419: "Stability of Calcium Sulfate Base Course in a Wet Environment"), different stabilization schemes were applied to raw BCS in order to improve its water susceptibility. Results of moisture sensitivity and unconfined compressive strength (UCS) tests indicated that BCS stabilized with either the grade 120 granulated ground blast furnace slag (GGBFS) or with GGBFS and some secondary stabilizers (Type I Portland cement, lime, or Class C fly ash) can achieve a significantly better performance than the raw BCS in terms of both water resistance and UCS strength *[2]*, *[3]*.

In order to verify the efficiency of laboratory derived BCS stabilization schemes and further assess related field performance and economic benefits of using stabilized BCS materials, an APT experiment was recently conducted at LTRC's pavement research facility (PRF) site using ALF. This APT experiment, titled "Accelerated Loading Evaluation of a Sub-base Layer on Pavement Performance," is the fourth APT experiment conducted at the PRF site (hereafter called this experiment as ALF 4). The overall test program of ALF 4 included six test sections with five different base materials. Figure 1 presents a plan view of ALF 4 test sections. Note that only the following three test sections will be included in this research

report: 4-1A with a slag stabilized BCS base course (hereafter called BCS/Slag), 4-2A with a fly ash stabilized BCS base course (hereafter called BCS/Flyash), and 4-1B with a crushed limestone base course.

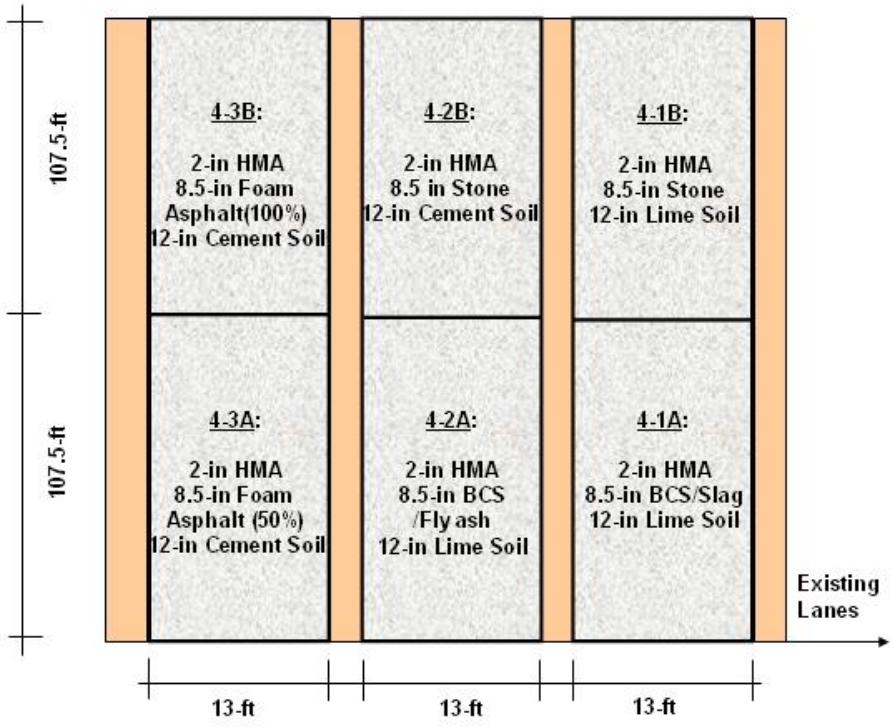

Figure 1
Plan view of ALF 4 test sections

All test sections of ALF 4 were constructed according to the *Louisiana Standard Specifications for Roads and Bridges* so that the project would be as representative as possible of actual highway construction practices *[1]*. A comprehensive field testing program was included during the construction. A detailed construction report as well as related field test results during the construction can be found in the Appendix of this report.

OBJECTIVE

The objectives of this research study were two-fold: (1) to evaluate field performance of stabilized BCS base materials as compared to a crushed stone base course under accelerated loading and (2) to assess economic benefits of using stabilized BCS materials in lieu of a stone base course.

SCOPE

Accelerated loading of three full-scale APT test sections was the main scope of this study. It included field instrumentation for monitoring moving-load induced pavement responses, non-destructive testing using both falling weight deflectometer (FWD) and Dynaflect, surface distress survey, and evaluation of pavement structural performance of tested sections. Based on the accelerated loading results, potential cost benefits of using stabilized BCS base materials were quantified through both the construction cost and life cycle cost analyses.

METHODOLOGY

Description of APT Test Sections

Pavement Structures

Figure 2 presents pavement structures for the three APT test sections considered in this study. As shown in Figure 2, each section included a 2.0-in. hot mix asphalt (HMA) wearing course, an 8.5-in. base course, and a 12-in. lime-treated working table layer over an A-6 embankment subgrade. Except for the different base materials, the three test sections were constructed with the same materials for all other pavement layers. Because the focus of this study was the performance of different base courses, only a 2.0-in. thin HMA wearing course was used. The base courses for sections 4-1A, 4-2A, and 4-1B were BCS/Slag, BCS/Flyash, and crushed stone, respectively. Also outlined in Figure 2 is the field instrumentation layout on each test section, which will be discussed in a subsequent section.

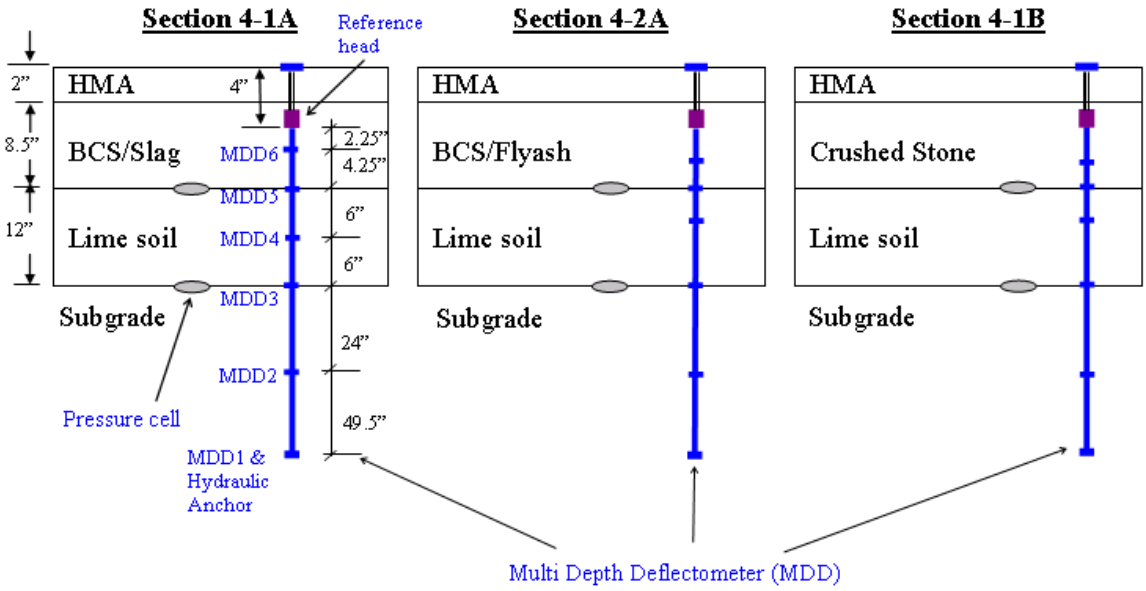

Figure 2
Pavement structures of ALF test lanes

Materials

HMA Mixture. The HMA mixture used was a ¾-in. nominal maximum size Superpave mixture designed at a compaction effort of 100 gyrations using the Superpave Gyratory Compactor. The aggregate blend consisted of 45.4 percent #67 coarse granite aggregate, 17.1 percent #11 crushed siliceous limestone, 10.3 percent coarse sand, 12.9 percent crushed gravel, and 14.3 percent reclaimed asphalt pavement (RAP). The optimum asphalt binder content was 4.4 percent including 3.7 percent PG 76-22 M virgin binder (elastomeric polymer-modified) and 0.7 percent recycled binder (from RAP).

Stabilized BCS Bases. The raw BCS material used in this study was supplied by Bear Industries Inc., Port Allen, LA. This material had a pH value of 6.5 and its chemical components are listed in Table 1.

Table 1
Chemical composition of BCS *[2]*

Compositions	Percentage by weight
SiO_2	0.5
Al_2O_3	0.1
Fe_2O_3	0.2
CaO	29.0
SO_4	54.0
CO_3	3.0
Moisture	5-30

As shown in Figure 2, section 4-1A had a grade 120 GGBFS stabilized BCS base (BCS/Slag) with 10 percent by volume, and section 4-2A used a 15 percent by volume Class C fly ash stabilized BCS base (BCS/Flyash). The two chemical stabilizers – GGBFS and Class C fly ash – were supplied by Buzzi Unicem USA of New Orleans and Bear Industries, Inc., respectively. The chemical components are listed in Table 2.

Table 2
Chemical composition of slag and fly ash *[2]*

Composition (%)	GGBFS	Class C Fly Ash
SiO2	34.5	47.5
Al2O3	9.5	4.1
Fe2O3	1.3	5.2
CaO	39.6	20.1
MgO	10.9	2.5
K2O	1.3	0.7
Na2O	0.5	0.3

During construction, a sufficient amount of loose stabilized-BCS material was collected immediately after it was thoroughly mixed in the field. Several field core samples were taken from the stabilized BCS layers 35 days after the base course construction *[2]*. As shown in Figure 3, laboratory results indicated that the addition of slag in BCS changed the particle size distribution as compared to raw BCS materials; whereas, the addition of Class C type fly ash did not.

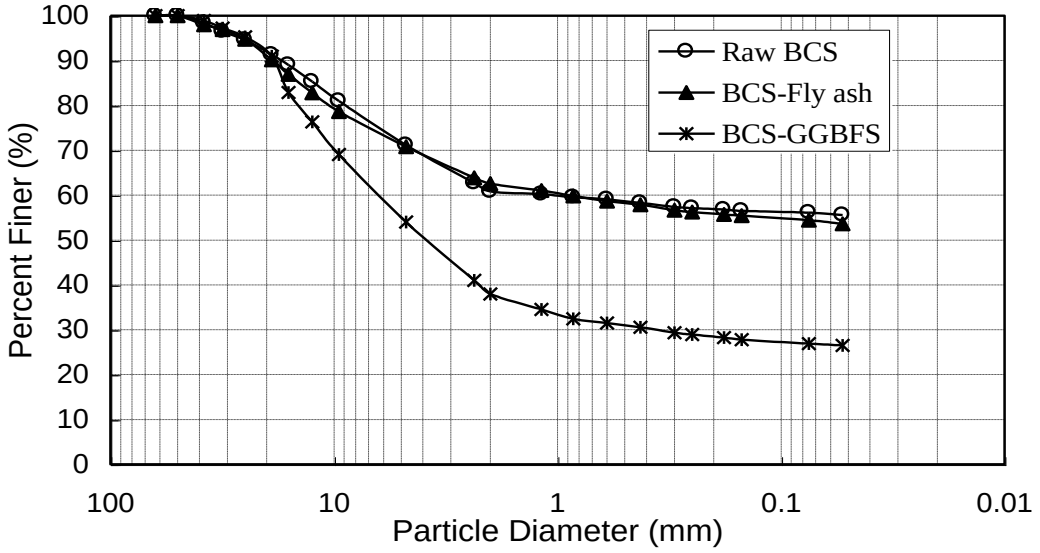

Figure 3
Particle size distribution of non-stabilized and stabilized BCS *[2]*

Field cores were further tested in the laboratory for moisture sensitivity *[2]*. As shown in Figure 4, after submerging in water for four hours, a BCS/Slag core remained in a solid

condition; whereas, a BCS/Flyash core had fallen apart in pieces. This indicates that the BCS/Flyash base may be moisture-susceptible under a wet condition; whereas, the BCS/Slag base may not.

(a) BCS/Flyash after 4 hrs water soaking

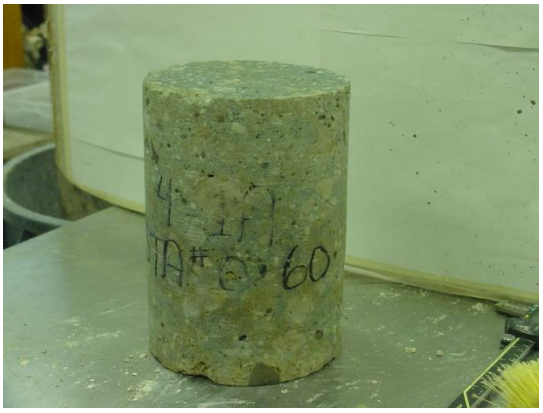

(b) BCS/Slag after 4 hrs water soaking

Figure 4
Core pictures of BCS/flyash and BCS/slag *[2]*

Crushed Limestone. The crushed stone base of section 4-1B was a control base course in this experiment, constructed as a Class-II base course according to LADOTD's Standard Specification for Roads and Bridge *[1]*. Kentucky crushed limestone was used. The corresponding gradation specification requirements for Class-II stone base are listed in Table 3. Note that the maximum liquid limit and the maximum plasticity Index of a Class-II base course shall be less than 25 and 4 percent, respectively, for the fraction of stone passing the No. 40 sieve *[1]*.

Table 3
Gradation specification requirements for Class-II stone base *[1]*

U.S. Sieve	Percent Passing
1½ in.	100
1 in.	90~100
¾ in.	70~100
No. 4	35~65
No. 40	12~32
No. 200	5~12

Lime-Soil Layer and Subgrade. The lime soil layer shown in Figure 2 is a lime treated "working table" layer created for pavement construction. In this experiment a 12-in. lime-treated working table layer was constructed by field mixing of 10 percent lime by volume with the existing embankment subgrade soil (as classified to be an A-6 soil in the AASHTO classification). Table 4 presents physical properties of the soil. Basically, it is a silty-clay, consisting of 60.3 percent silt and 23.5 percent clay with a plastic index of 10.

Table 4
Soil properties

Passing # 200 (%)	Clay (%)	Silt (%)	LL (%)	PI	W_{opt} (%)	γ (kN/m^3)	Classification	
							USCS	AASHTO
91	23.5	60.3	31	10	18.5	17.1	CL-ML	A-6

Instrumentation

Field instrumentation of this study consisted of using multi-depth deflectometers (MDD) and earth pressure cells for measuring load-induced vertical deformations and compressive stresses. As shown in Figure 2, each test section was embedded with two Geokon 3500 pressure cells (one at the bottom of base layer and the other on the top of subgrade) and one MDD with six potentiometers. Note that the MDD station on each section was about 4.5 ft. away from that of the pressure cells along the centerline. A brief description of each instrumentation device and related data acquisition system is given below.

Pressure Cell. The Geokon model 3500 earth pressure cell [Figure 5(a)] is designed to measure total pressure in earth fills and embankments as well as other structures. The pressure cell has a range up to 100 psi. It has a 350-ohm resistance strain gauge type with a 10 volt maximum excitation. The pressure cell consists of two circular 9 in. diameter stainless steel plates welded contiguously around their periphery and spaced apart by a narrow cavity filled with an anti-freeze or mercury solution. A high pressure stainless steel tube connects to the plates with a pressure transducer placed in the cavity. External pressures acting on the cell are balanced by an equal pressure induced in the internal fluid. This pressure is converted by the pressure transducer into an electrical signal that is transmitted by a four conductor shielded cable to a readout location. The entire device weighs approximately 5 lb.

Multi-Depth Deflectometer. The MDD used is called SnapMDD^{TM}, a patented device manufactured by the Construction Technology Laboratories, Inc, Illinois. The SnapMDD is designed to measure both compressively elastic and plastic deformations up to

seven different depths throughout a pavement structure under traffic loading. It is installed through a bore hole on pavement surface with a typical dimension of 5 in. in diameter and 10 ft. in depth. The reference point for deformation measurements is 4 in. below pavement surface. Deformation sensors inside the MDD are individually wired – not serial, each of which has a 1-in. maximum electrical travel length under a 10-volt excitation. In this study, each MDD contains six deformation sensors, each installed at a distance from the surface of 6.25 in., 10.5 in., 16.5 in., 22.5 in., 46.5 in., and 96 in., respectively [Figure 5(b)].

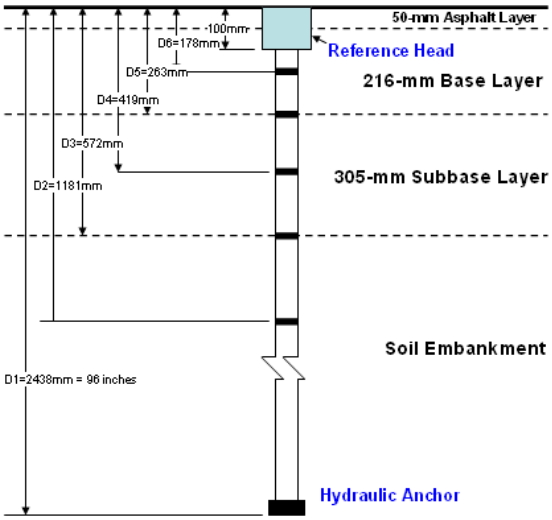

(a) **(b)**

Figure 5
(a) Geokon model 3500 earth pressure cell; (b) MDD sensor locations

Data Acquisition System. The Megadac 3415A data acquisition system is used in this study. It has up to 512 channels and 64 megabytes of internal non-volatile onboard memory. The signal conditioning provides for quarter, half and full bridge operation, programmable gain up to 4,000, eight pole Butterworth filtering, auto balance, auto zero and voltage calibration. In this study, the sampling rate selected was 1,000 per second for both instrumented devices.

Laboratory Material Characterization

Laboratory tests were conducted to determine general properties of BCS and to investigate the mechanism responsible for the strength deterioration of raw BCS in a wet environment. The basic properties of BCS mixtures were determined through the gradation analysis, specific gravity test, and moisture-density compaction curves with various compaction energy. The strength properties of BCS were captured by unconfined compressive strength (UCS) tests. The detailed test results have been published in the LTRC Final Report 419 *[2]*. In addition, two repeated load triaxial tests were used to characterize the resilient and permanent deformation properties of different base materials considered in this study, which are briefly described below.

Resilient Modulus Test

The resilient modulus test was performed on the base materials according to the AASHTO T-307-99 test method *[6]*. The resilient modulus test is a triaxial cell based repeated load test using a MTS loading machine and cylindrical samples with a dimension of 6 in. in diameter and 12 in. in height. During a test, each loading cycle consisted of a haversine load pulse of a 0.1-second loading and a 0.9-second resting period. Multiple combinations of various confining and deviatoric stresses were applied on one sample for numbers of cycles to complete one test. Details of the resilient modulus testing have been reported elsewhere *[6]*. In this study, the constitutive soil model, recommended by the NCHRP project 1-37A for the use in the new Mechanistic-Empirical Pavement Design Guide (MEPDG), was employed to analyze the test results, which has the following form *[9]*:

$$\frac{M_r}{P_a} = k_1\left(\frac{\theta}{P_a}\right)^{k_2}\left(\frac{\tau_{oct}}{P_a}+1\right)^{k_3} \qquad (1)$$

where,

M_r = resilient modulus,

θ = bulk stress = $\sigma_1+\sigma_2+\sigma_3$,

σ_1 = major principal stress,

σ_2 = intermediate principal stress= σ_3,

σ_3 = minor principal stress/ confining pressure,

$\tau_{oct} = \frac{1}{3}\sqrt{(\sigma_1-\sigma_2)^2+(\sigma_1-\sigma_3)^2+(\sigma_2-\sigma_3)^2}$,

P_a = normalizing stress (atmospheric pressure) = 14.7 psi, and

k_1, k_2, k_3 = material constants.

Permanent Deformation Test

A permanent deformation test was also performed on the base materials according to a test procedure similar to the AASHTO T 307 test *[6]*. The same loading pulse and cylindrical samples were used in permanent deformation tests as the resilient modulus tests. However, only one selected combination of vertical stress and confining pressure was applied to the samples for 10,000 cycles. A relationship between the plastic strains and loading cycles can be obtained from the permanent deformation test.

Description of Accelerated Loading Experiment

ALF Loading History

The APT loading device used is called the ALF (Accelerated Loading Facility). The ALF wheel assembly models one half of a single axle and the load is adjustable from 9,750 lb. to 18,950 lb. per load application. The dual tires mounted on the ALF machine (Figure 6) were the Michelin radial 11R22.5 tires, inflated to 105-psi cold. The load magnitude of the ALF dual tires may be adjusted (increased) by adding one or more steel loading plates (each weighs 2,300 lb).

Figure 6
Louisiana ALF with dual tires

As mentioned before, six test sections were included in ALF 4 (Figure 1). The ALF loading for the entire APT experiment was divided into two loading phases: phase one was to test three "A" sections, and phase two was for loading on three "B" sections. During each phase of loading, the ALF device was moved alternatively from one section to another after every 25,000 ALF passes. Note that this APT experiment was conducted under a natural southern

Louisiana highway condition without any environment confinement. A 15-in. traffic wander was used during the testing.

Each testing phase lasted approximately one year. The beginning ALF wheel load was 9,750 lb. (i.e., the self-weight of ALF's wheel assembly). The magnitude of wheel load was then increased gradually by adding one additional steel load plate of 2,300 lb. at different designated loading cycles. The applied load history (i.e., the sequence in terms of loading cycles at which an additional steel load plate was added to the ALF device) was kept the same in both testing phases. Since different sections would be failed at different number of ALF passes, Figure 7a presents the longest ALF loading history of this experiment. The ALF loading history was also converted into an 18,000-lb. equivalent single axial load (ESAL) based on the fourth power law, Figure 7b. Since only sections 4-1A, 4-2A, and 4-1B were included in this study, Tables 5-7 list the loading sequence in terms of ALF passes applied on each test section considered.

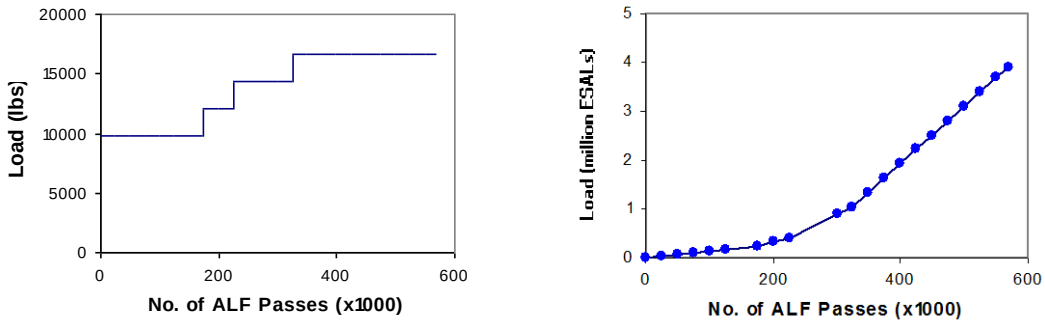

(a) **(b)**

Figure 7
ALF loading history

Table 5
ALF passes applied to section 4-1A

No. of Passes (x 1000)	Total Load lb.	ESAL Factor	ESALs	Cumulative ESALs
0 – 175	9,750	1.377	241,039	241,039
175 - 225	12,050	3.213	160,674	401,713
225 - 325	14,350	6.463	646,306	1,048,019
325-575	16,650	11.713	2,928,377	3,976,396

Table 6
ALF passes applied to section 4-2A

No. of Passes (x 1000)	Total Load lb.	ESAL Factor	ESALs	Cumulative ESALs
0 - 175	9,750	1.377	241,039	241,039
175 - 225	12,050	3.213	160,674	401,713
225 - 325	14,350	6.463	646,306	1,048,019
325-505	16,650	11.713	2,108,431	3,156,450

Table 7
ALF passes applied to section 4-1B

No. of Passes (x 1000)	Total Load lb.	ESAL Factor	ESALs	Cumulative ESALs
0 - 175	9,750	1.377	241,039	241,039

Failure Criteria

For this experiment, a test section was considered to have failed when the pavement condition met one of the following failure criteria, whichever came first: (1) the average rut depth reached up to 0.5 in. among eight measurement stations within the trafficked area of a section or (2) 50 percent of the trafficked area of a section developed visible cracks (e.g., longitudinal, transverse, and alligator cracks) more than 1.5 ft/ft^2.

Field Measurements

The field instrumentation data were collected at approximately every 8,500 ALF load repetitions. All pavement responses were measured under the left tire of the ALF dual tire assembly when the tire was directly positioned on the top of an instrumentation device (i.e., pressure cell and MDD).

Non destructive tests (NDT) including Dynaflect and falling weight deflectometer (FWD) as well as the rutting and cracking survey were performed at the end of each 25,000 load repetitions. The effective loading area of ALF testing is about 32-ft. long in which deflection measurements and distress survey were taken at eight stations of 4-ft. intervals.

The FWD device used in this study was a Dynatest 8002 model FWD device. The surface deflections were measured with nine sensors spaced at 0, 8, 12, 18, 24, 36, 48, 60 and 72 in., respectively. The Dynaflect is another surface deflection measurement device. This device induces a dynamic load of 1,000 lb. at a frequency of 8 Hz on the pavement and measures the resulting deflections by using five geophones spaced under the trailer at approximately 1-ft. intervals from the application of the load.

Data Analysis Techniques

The data analysis of this study include the processing of NDT deflection data, evaluation of instrumentation results, modeling pavement structure, and prediction of pavement performance in terms of pavement distresses. The following analysis procedures and software are used in this study.

Dynaflect-Deflection Based Pavement Evaluation Chart

Kinchen and Temple developed a Louisiana pavement evaluation chart for the estimation of existing pavements' structural number based on Dynaflect measured deflection *[7]*. As shown in Figure 8, an effective structural number and a design subgrade modulus of existing pavements can be determined based on a temperature-corrected Dynaflect center deflection and a percent spread value. The percent spread (*Sp*) is the average deflection in percentage of the central deflection:

$$Sp = \frac{D_0 + D_{300} + D_{600} + D_{900} + D_{1200}}{5 \times D_0} \times 100\, percent \qquad (2)$$

where,
D_{300}, D_{600}, D_{900}, and D_{1200} = deflections measured at 12 in., 24 in., 36 in. and 48 in. from the center of the applied load.

This method was used in the analysis of Dynaflect deflection results for determination of the effective structural number of test sections under different ALF repetitions.

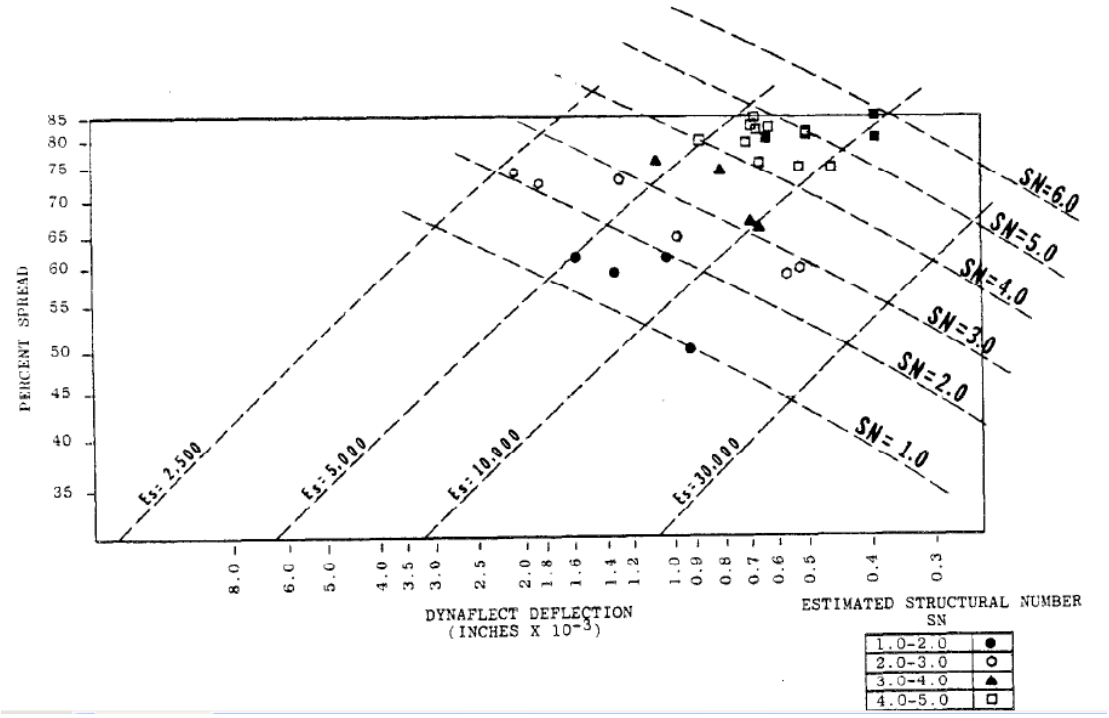

Figure 8
Louisiana pavement evaluation chart *[7]*

EVERCALC

The EVERCALC is a windows-based computer program developed by Washington DOT for backcalculation of layer moduli based on FWD measured deflection basins *[8]*. EVERCALC is based on the multilayered elastic analysis program, WESLEA (provided by the Waterways Experiment Station, U.S. Army Corps of Engineers), which produces the pavement response parameters, such as stresses, strains, and deformations in the pavement system. EVERCALC was used in this study for the backcalculation of layer moduli based on FWD measured deflection bowls.

During the backcalculation process, primarily due to the very thin asphalt top layer (2-in.) used in pavement test sections, directly using a four-layer pavement structure as those shown

in Figure 2 could not back-calculate a set of reasonable modulus values based on any FWD deflection bowls measured. In fact, very large root mean square (RMS) errors were observed on trials of many FWD deflections. In addition, the EVERCALC program tends to provide a very high modulus value (generally higher than 290 ksi) for the lime treated soil layer used in test sections. The modulus value of 290 ksi is significantly higher than those obtained in laboratory testing on this type of material (a range from 25 to 50 ksi). In order to obtain a relatively realistic set(s) of layer modulus for base and other materials, the elastic modulus of HMA layer was set to a fixed value of 725 ksi at 68°F in all FWD backcalculations.

ELSYM5

ELSYM5 was originally developed by Gale Ahlborn of the Institute of Transportation and Traffic Engineering (ITTE) at the University of California at Berkeley. It is based on the multi-layer elastic computer model, with the ability to consider multiple loads as well as the presence of a rigid base below the subgrade. ELSYM5 was used in computing the vertical stresses developed in the pavement section under the ALF load.

MEPDG

The Mechanistic-Empirical Pavement Design Guide (MEPDG) software Version 1.0, developed under NCHRP projects 1-37A and 1-40D, was used in this study to predict the permanent deformation development on the three test sections evaluated. A conventional flexible pavement cross-section similar to the ones shown in Figure 2 was used in the analysis. The structure is a four-layer pavement system with a single 2-in. thick asphalt concrete layer, an 8.5-in. thick stabilized base layer, a 12-in. thick treated soil layer, and an infinite subgrade. In general, the laboratory resilient modulus test information was used as design inputs for the permanent deformation development analysis. As pointed out in the MEPDG software, the use of Level 1 input [k_1, k_2, k_3 values in equation (1)] for the base, subbase, and subgrade layers is not recommended at this time because Level 1 inputs utilized the stress dependent finite element method, which has not been calibrated with distress. Therefore, Level 2 inputs were chosen for all pavement layers (other than the asphalt layer) based on the laboratory resilient modulus test results; whereas, the Level 3 input was selected for the asphalt concrete layer for simplicity. In order to best simulate the traffic load applied on each APT test section, different initial two-way average annual daily truck traffic (AADTT) were assumed with 50 percent of trucks in the design direction and 100 percent of trucks in the design lane. Table 8 presents the details of APT traffic inputs. The vehicle classification file was modified to only include 18,000 lb. single axle trucks with an axle configuration similar to the ALF load machine. Such traffic inputs would result in various numbers of cumulative heavy trucks (or 18,000 lb. ESAL) at the end of the 1-year design life, which are very close to the total ESAL repetitions in different APT test sections. In

addition, the “loading months” in Table 8 simulates the actual time of each test lane in this study. The environmental file was generated from the Baton Rouge weather station database included in the MEPDG software.

Table 8
APT traffic inputs used in MEPDG analysis

Section	Load Begin	Load End	ESAL	Load Months	AADTT	Design Life
4-1A	Oct-05	Oct-06	3,913,849	13	9,898	1 Year
4-2A	Oct-05	Sep-06	2,349,018	12	6,436	
4-1B	Jan-07	Apr-07	120,954	4	994	

DISCUSSION OF RESULTS

Results presented for discussion included laboratory RLT tests, field non-destructive deflection measurements, instrument responses to vehicular loading, surface distress survey, and forensic investigation on failed pavement structures. In addition, the pavement rutting performance was analyzed using the newly developed MEPDG software, and the structural layer coefficients for the two chemically stabilized BCS base materials used in this study were quantitatively estimated based on the APT performance results. Finally, economic benefit analyses were performed on different pavement alternatives to address the potential cost saving of using the recommended BCS/Slag base materials in lieu of a stone base.

Laboratory RLT Test Results

Resilient Modulus Test Results

Table 9 presents the resilient modulus test results for the three base materials used in the test sections. The k-values in Table 9 are the required level-1 inputs in MEPDG, which was determined by fitting the resilient modulus test results at varied bulk and deviator stresses into equation (1) *[9]*. The last column in Table 9 provides the typical resilient modulus (M_r) values under an estimated in-situ load induced stress condition (i.e., bulk stress is 15 psi and deviator stress is 5 psi). Note that the cylindrical samples were fabricated using loose materials mixed in the field and collected during construction. Therefore, the moisture content of the prepared samples represents in-situ material moisture condition at construction.

Table 9
Resilient modulus test results

Material	k1	k2	k3	M_r (ksi)
BCS/Slag	8114	0.27	-0.08	123.3
BCS/Flyash	5950	0.22	-0.30	87.7
Crushed Stone	2131	0.55	-0.34	39.1

Among the coefficients, k_1 is proportional to Young's modulus and has been considered as the best indicator of the stiffness characteristics of the base and subgrade layers by many researchers *[10]*, *[11]*. Thus, by referring to those k_1 and typical M_r values in Table 9, the following observations were made: (1) BCS/Slag is stiffer than BCS/Flyash; (2) both stabilized BCS materials are considerably stiffer than the crushed stone.

Permanent Deformation Test Results

Permanent deformation characteristics for the stabilized BCS materials and the crushed stone are shown in Figure 9 by plotting permanent strain versus repeated load cycles. Generally, the permanent deformation of a tested sample continues to grow as repeated loading proceeds, but at gradually decreasing rates. As seen in Figure 9a, the permanent strain of the crushed stone base increased significantly faster than both BCS materials, indicating its weak resistance to permanent deformation. On the other hand, the fly ash-stabilized samples underwent a larger permanent deformation than the slag-stabilized samples, since their averaged permanent deformation was about three times as large as those of the slag-stabilized BCS, Figure 9b. Overall, the final permanent strains of the three tested materials ranged from 0.005 percent of BCS/Slag to 0.016 percent of BCS/Flyash and 0.295 percent of the crushed stone. In terms of rut resistance, the ranking order for the three base materials from high to low is BCS/Slag, BCS/Flyash, and crushed stone.

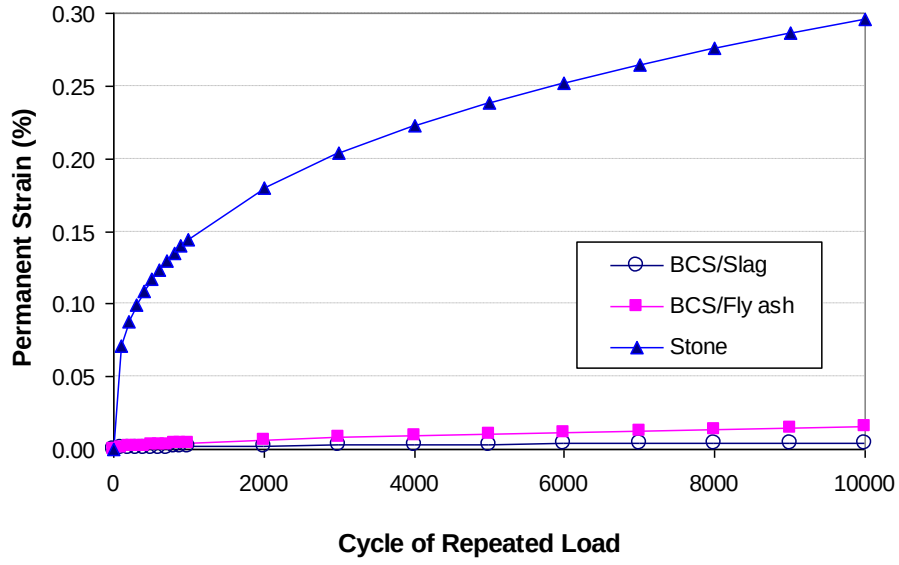

(a)

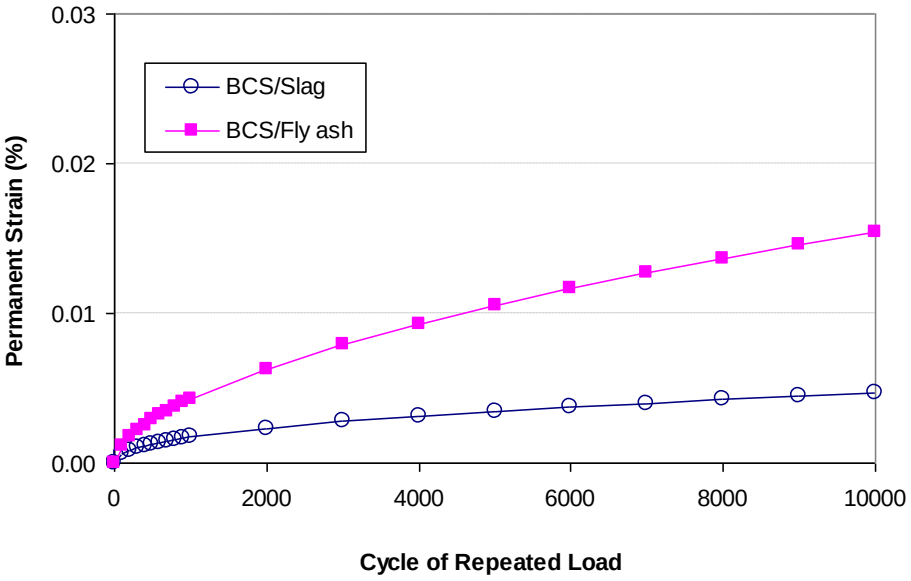

(b)

Figure 9
Permanent deformation of stabilized BCS vs. stone

Non-Destructive Test Results

Pavement surface deflections were measured during the ALF testing by both Dynaflect and FWD methods on each test section at an interval of every 25,000 ALF repetitions.

Pavement Structural Capacity Estimated from Dynaflect Test Results

Figure 10 presents ALF load induced progression of the average structure number (SN) values for the three test sections evaluated, which were estimated by applying the Dynaflect measured deflections into the Louisiana Pavement Evaluation Chart. A higher SN value indicates a greater structural capacity of a pavement. An initial increase in the SN values during the first 50,000 ALF passes or so may be attributed to the post construction densification of pavement layers and the corresponding material strength gains due to the curing. As expected, the overall SN values generally displayed a slightly decreasing trend (due to pavement deterioration) with the increase of load repetitions. It was noticed that some severe localized surface cracks developed in section 4-1B after 75,000 ALF repetitions; whereas, no cracks were observed on other two test sections.

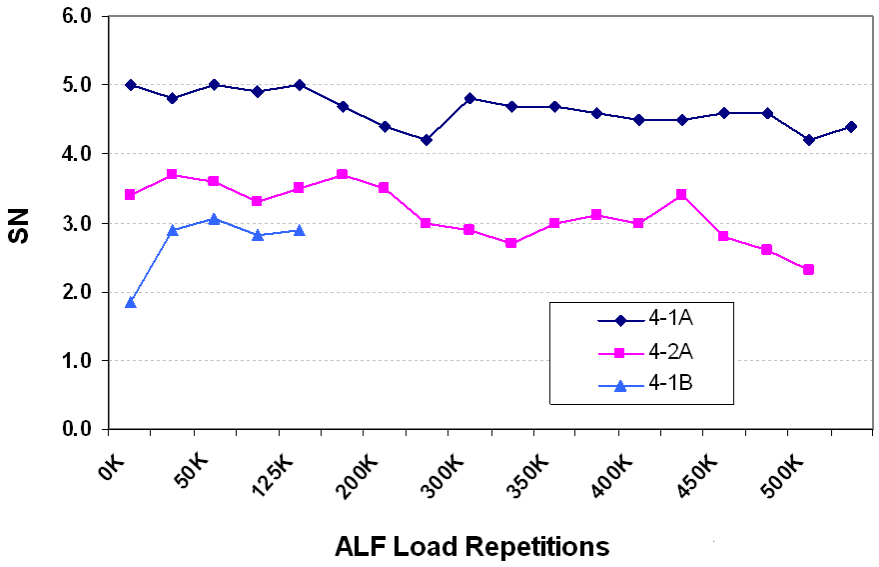

Figure 10
Dynaflect structural number results

In general, section 4-1A with a BCS/Slag base layer possessed the highest SN values among the three sections tested, followed by section 4-2A with a BCS/Flyash base. The lowest SN values were observed in section 4-1B, which had a crushed stone base layer. Since the only difference among test sections is the base course materials, it may be deduced from Figure 10 that (1) the in-situ SN value of the 8.5-in. BCS/Slag base in section 4-1A was at least 1.0 SN

value higher than the BCS/Flyash base in section 4-2A and (2) the in-situ structural number of the stone base in section 4-1B was approximately 0.5 SN value lower than the BCS/Flyash base. A higher SN value implies a larger structural layer coefficient value for the stabilized BCS materials (SN = layer coefficient x 8.5-in. layer thickness).

FWD Test Results

Figure 11 presents the average FWD center deflection (D0) test results for the test sections evaluated. The deflection was first normalized to a 40-kN load level and then temperature-corrected to 25^{o}C based on a procedure developed under the Long Term Pavement Performance (LTPP) program *[12]*. The center deflection measured directly under the FWD loading plate is usually considered as an indicator of the composite stiffness of a pavement structure. A higher surface deflection indicates a smaller composite stiffness for a pavement structure. The initial decrease of D0s in Figure 11 is presumably due to the post-compaction of pavement layers and the curing of base and subbase materials. The appearance of Figure 11 indicates that the D0s of section 4-1A were significantly less than those on sections 4-2A and 4-1B; whereas, sections 4-1B had much greater D0s than those of section 4-2A. Overall, the normalized D0 results were found consistent with the Dynaflect structure number results shown in Figure 10.

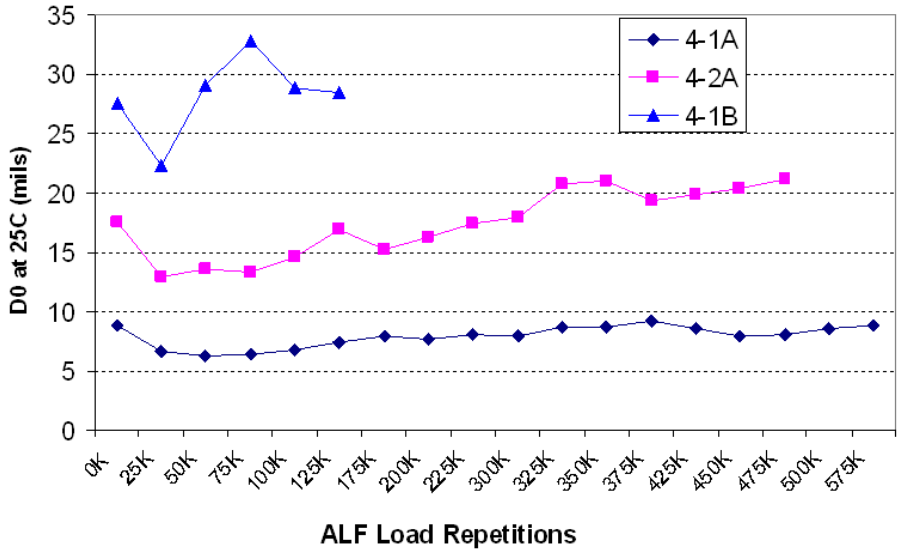

Figure 11
FWD center deflections

Tables 10 through 12 present FWD backcalculation results for sections 4-1A, 4-2A, and 4-1B, respectively. It is noted that, in order to obtain a more realistic set of backcalculated layer moduli with acceptable RMS errors during the FWD backcalculation process, section 4-1A was modeled as a three-layer system (2 in. HMA + 8.5 in. BCS/Slag + a combined subgrade); whereas, section 4-2A and 4-1B were modeled as a four-layer system as the pavement structures shown in Figure 2. In general, the FWD backcalculation RMS errors of section 4-2B were less than 3 percent, followed by section 4-1A of less than 5 percent, and less than 10 percent was for section 4-2A.

Table 10
FWD backcalculation moduli for section 4-1A

No. of Passes x 1000	Cumulative ESALs x1000	Modulus (ksi)		
		HMA	BCS/Slag	Combined Subgrade
0K	0	627.7	2733.6	22.3
50K	69	747.8	2561.1	26.0
75K	103	935.5	2541.8	25.7
125K	172	531.8	1926.4	21.6
175K	241	521.6	1724.2	19.6
200K	321	578.9	1762.5	20.6
225K	402	556.9	1718.6	19.6
250K	482	413.2	1582.6	18.3
300K	886	542.1	2152.7	21.1
325K	1048	429.2	1502.5	20.0
350K	1341	413.4	1377.8	20.4
375K	1634	484.7	1299.2	20.6
425K	2219	527.6	1232.3	21.4
450K	2512	635.4	1509.4	22.3
475K	2805	632.3	1383.3	22.6
500K	3098	582.2	1299.0	21.5
575K	3976	737.6	1194.3	22.1

Table 11
FWD backcalculation moduli for section 4-2A

No. of Passes	Cumulative ESALs x1000	Modulus(ksi)			
		HMA	BCS/Flyash	Lime Soil	Subgrade
0K	0	758.0	73.9	44.1	20.2
25K	34	756.3	166.8	52.3	24.6
50K	69	902.1	134.1	54.8	25.7
75K	103	751.1	149.6	53.7	24.6
125K	172	706.2	81.7	50.2	22.8
175K	241	572.3	134.1	44.0	20.0
200K	321	605.0	99.3	43.2	19.6
225K	402	577.4	85.8	41.6	18.5
250K	482	544.3	97.9	39.0	17.3
300K	886	570.2	130.3	44.7	19.4
325K	1048	565.7	72.5	41.6	17.8
350K	1341	659.0	80.5	40.0	17.0
375K	1634	682.3	72.5	42.5	18.1
425K	2219	805.2	62.5	44.4	18.9
450K	2512	1423.8	45.8	45.7	19.3
500K	3098	1396.5	48.2	44.4	18.8
505K	3156	455.4	47.1	34.3	12.6

Table 12
FWD backcalculation moduli for section 4-1B

No. of Passes	Cumulative ESALs x1000	Modulus (ksi)			
		HMA	Crushed Limestone	Lime Soil	Subgrade
0K	0	965.9	54.4	84.9	20.1
25K	34	738.2	74.2	60.0	17.1
50K	69	581.0	82.4	65.9	16.7
75K	103	525.8	81.3	61.7	16.3
100K	138	632.2	81.1	54.6	16.7
125K	172	600.7	55.7	86.8	16.7

Figure 12 presents the backcalculation results for the three base materials considered. As can be seen in the figure, all three materials showed a decreasing trend in stiffness as ALF load repetitions increase, presumably due to material deterioration under trafficking. The BCS/Slag base had a significantly higher in-situ modulus (>10 times) than both BCS/Flyash and crushed stone, while the modulus of BCS/Flyash was about two times greater than that of the stone. The FWD backcalculation results indicated that in-situ modulus of a BCS/Slag

layer could be achieved higher than the modulus of a HMA layer, which resulted in an inverted pavement structure for section 4-1A.

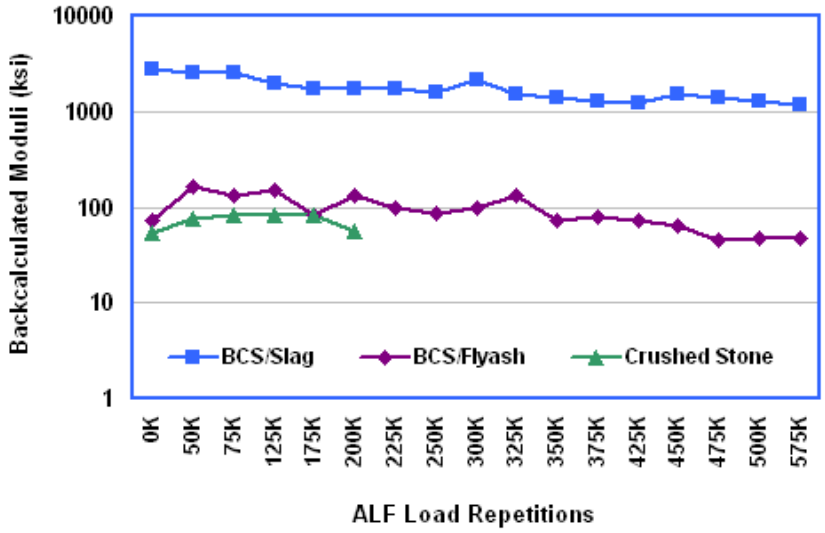

Figure 12
Backcalculated moduli of base materials

The FWD backcalculation results indicate that (1) BCS/Slag had a significantly higher in-situ modulus than both BCS/Flyash and crushed stone; (2) both sections of 4-1A and 4-2A showed a drop in the stabilized BCS base modulus after trafficking usually attributed to the internal material degradation (e.g., developing load-induced micro-cracks); (3) no degradation seemed to be occurred on the stone base in section 4-1B (this may be due to the very short load period with much less load repetitions received by this section); and (4) the backcalculated moduli of lime soils were found to have a range from 40 to 90 ksi. However, due to having different base materials, section 4-1B appeared to have a higher in-situ modulus for the lime-soil layer than section 4-2A.

Instrument Responses to ALF Wheel Loading

Pressure Cells

Figure 13 presents the typical stress signals of both base and subbase pressure cells measured under the 9,750-lb. ALF wheel load. The sampling rate in the data acquisition was 1,000 recordings per second and signals shown in Figure 13 for both pressure cells are judged to be

good. As expected, the measured vertical stresses were higher in the base pressure cell than that in the subbase pressure cell (Figure 13). As shown in the rescaled portion in Figure 13, it is also noticed that the subbase pressure cell has a wider but flatter bell-shape signal than the base pressure cell. This does make sense because the surface wheel load is distributed at a certain spread angle from top to bottom in a pavement structure. When the ALF wheel load was approaching to the pressure cell station, it would first influence the subbase pressure cell due to its wider load influence zone at a deeper depth (i.e., the subbase pressure cell was placed at a depth 12 in. below the base pressure cell).

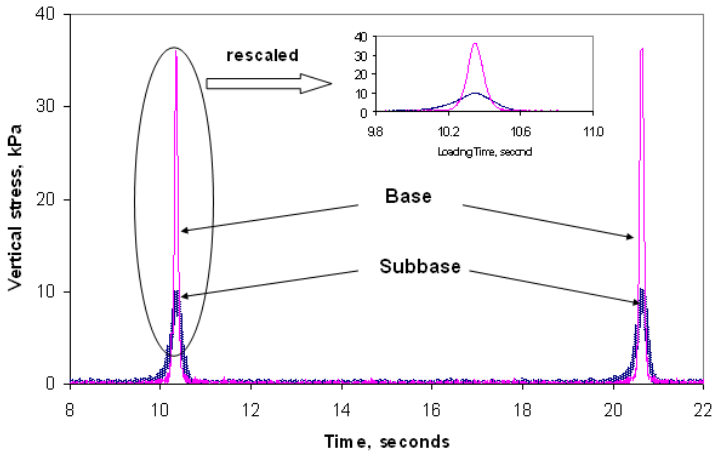

Figure 13
Typical measured vertical stresses under wheel loading

Table 13 presents a statistical summary of measured vertical compressive stresses obtained from two pressure cells installed on each test section. Only the pressures measured under a 9,750-lb. ALF moving load were listed in Table 13. This was because section 4-1B was failed under this load and the responses of the three test sections need to be directly compared. As shown in Table 13, under a dual tire load of 9,750-lb., the average vertical compressive stresses at the bottom of base layers were 0.9, 5.2, and 34.0 psi for sections 4-1A, 4-2A, and 4-1B, respectively, whereas, those values on top of a subgrade were 0.5, 1.8, and 0.6 psi, respectively. Such results indicate that the stiff BCS/Slag material in section 4-1A showed a significantly larger load spreading angle than the other two base materials. In addition, the BCS/Flyash base in section 4-2A also distributed the load better than the stone base in section 4-1B. As stated earlier, data was collected roughly at every 8,500 load repetitions. The coefficient of variation (COV) shown in Table 13 may be related to the variation of pavement responses (vertical compressive stresses) due to the combination effects of seasonal variations (e.g., temperature and moisture) and pavement material deterioration under trafficking. In general, the highest COV value was found for the measurement on top of the subgrade layer in section 4-1B (the stone base section).

Table 13
Results of the measured vertical compressive stresses

Section	Statistics	Vertical Stress (psi)	
		At Bottom of Base	At Bottom of Subbase
4-1A	Avg	0.9	0.5
	Std	0.1	0.1
	COV	13%	14%
4-2A	Avg	5.2	1.8
	Std	0.5	0.2
	COV	10%	10%
4-1B	Avg	34.0	0.6
	Std	8.6	0.2
	COV	12%	34%

The measured vertical compressive stresses were further compared to those analytical values estimated from a multi-layer elastic analysis program, ELSYM5. Backcalculated moduli obtained from an initial FWD test were used in the analysis. Table 14 presents the measured and calculated vertical compressive stresses on the three lanes tested.

Table 14
Comparison of measured and calculated vertical compressive stresses

	Vertical Stress @ bottom of Base (psi)		Cal./Meas.	Vertical Stress @ bottom of Subbase (psi)		Cal./Meas.
	Measured	Calculated		Measured	Calculated	
4-1A	0.9	3.5	3.8	0.5	1.8	3.5
4-2A	5.2	10.9	2.1	1.8	3.4	1.9
4-1B	34.0	13.8	0.4	0.6	3.3	5.5

As shown in Table 14, stress ratios between the calculated and the measured generally ranged from 0.4 to 5.5, with both the highest and lowest ratios falling in the stone test section (section 4-1B). The discrepancy between the predicted and the measured values is certainly due to the limitations of using the multi-layer elastic theory. However, it is interesting to notice that, in Table 14, only the calculated vertical stress at the bottom of the stone base in section 4-1B was found smaller than the measured one; whereas, in all other cases, the predicted values were higher. Previous studies did show that, on the basis of the elastic layer theory, the calculated vertical stress at the bottom of unbound aggregate bases is generally half of the measured value *[13]*, *[14]*. This seems to match well with the results obtained from the stone base in this study. However, the question is why the elastic layer theory only

overpredicted vertical stress values for a stone base. The answer for this question may be illustrated by analyzing the predicted stress and strain distribution using the elastic layer theory. Figure 14 presents the predicted stresses and strains at top and bottom of both base layers in sections 4-1A and 4-1B estimated using ELSYM5.

As shown in Figure 14a, a tension zone (based on the predicted tensile strains) goes from somewhere inside the BCS/Slag base layer of section 4-1A. However, Figure 14b shows that the same tension zone in Section 4-1B will start from the middle of the HMA layer and then go all the way to the bottom layers. This indicates that the entire stone base layer is predicted under a tension zone in which large tensile strains are developed in both x-y directions (see ε_x and ε_y in Figure 14b). In reality, a stone layer cannot resist any significant tension because the material is unbound. If a stone aggregate layer received a large tension, the stone particles would begin to separate from each other. Therefore, the possible segregation of stone particles due to tension may explain why a higher than theory-predicted vertical stresses could be measured from an unbound base layer, such as the stone layer in section 4-1B. On the other hand, as shown in Figure 14a, only the bottom part of the BCS/Slag layer would be predicted under a small tension. Such tension should not easily cause a particle separation because the BCS/Slag is a bound material, which can somewhat endure tensile strains.

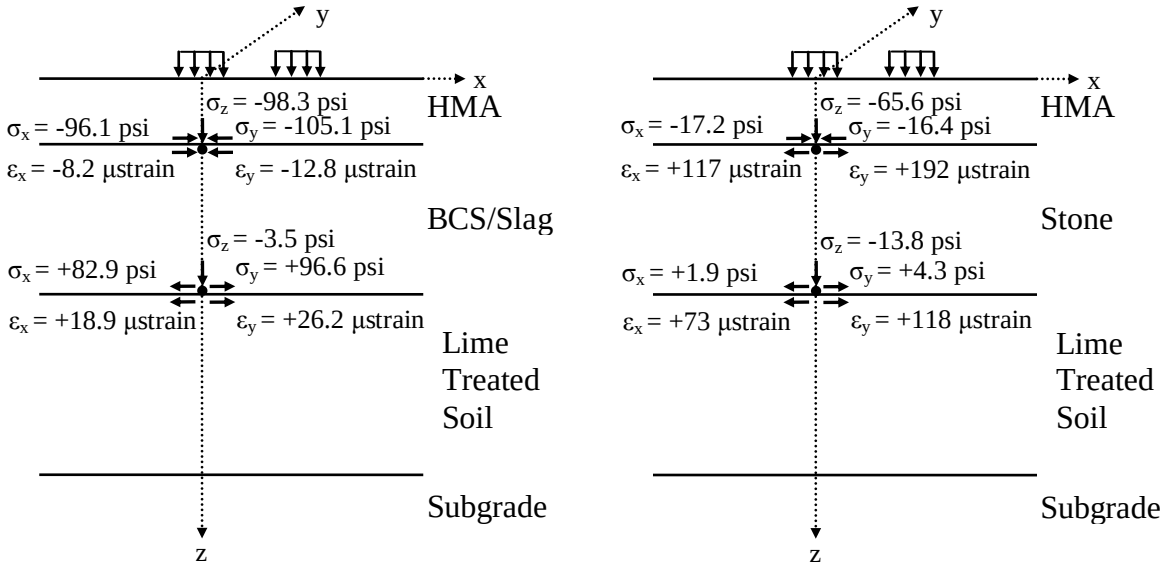

Figure 14
Stress and strain predictions. ("+" tension, "-" compression)

Besides the limitation of a multi-layer elastic theory, the discrepancy between the predicted and the measured vertical compressive stresses in BCS/Slag and other bounded layers may be partially attributed to the limitations of the pressure cell used. As pointed out by Dunnicliff, if the pressure cell stiffness is less stiff than soil stiffness, the cell tends to under-register, which will result in a smaller pressure value *[15]*. In fact, the stiff BCS/Slag layer in section 4-1A seems to be an extreme example for this phenomenon. As its modulus is significantly higher than any other base layers, the predicted vertical stress was found about 3 times higher than the measured value, Table 14.

MDD Results

As mentioned before, the MDD used in this experiment is called SnapMDD^{TM}, manufactured by Construction Technology Laboratories, Inc., in Illinois. A professional staff from the company was sent to the APT test site for the MDD installation. However, the MDDs installed on sections 4-1A and 4-2A only lasted for about 225,000 and 340,000 load passes, respectively, before the MDD baselines started to move (early failure). MDD installed on section 4-1B survived until this section failed, but the total number of load repetitions on this section was only 175,000 ALF passes. Therefore, the MDDs installed on this experiment were considered partially successful. The possible reasons for this early failure may be attributed to the installation. During the APT testing, a relatively weaker pavement area was found around the MDD surface cap, and more pavement distresses (e.g., rutting and cracking) were observed in this area as the increase of ALF load repetitions. After a discussion with the installation personnel, it was thought that the following scenarios were possibly the causes for this phenomenon. To install a SnapMDD, a 5-in. diameter bore hole of 8-ft. deep was drilled from pavement surface. The reference head of SnapMDD was 4-in. below the surface. After placing the MDD surface cap, a 5-in. by 4-in. cylindrical void would have resulted from the MDD installation. Such a cylindrical void was possibly too big for a pavement structure with only a 2-in. HMA layer to hold under a heavy load. In addition, during the MDD installation (including boring and instrumentation wire trench cutting), a certain amount of water was found to have entered into the pavement. Such excess water might have weakened the base materials (e.g., stabilized BCS materials) around the MDD and thus resulted in a relatively weaker pavement area around the MDD surface cap.

MDD measures both elastic and plastic deformations. Figure 15 shows a plot of a typical deflection bowl (elastic deformation) obtained in this study. By selecting the peak elastic deformation values in Figure 15(a), a deflection profile can be obtained, as shown in Figure 15(b).

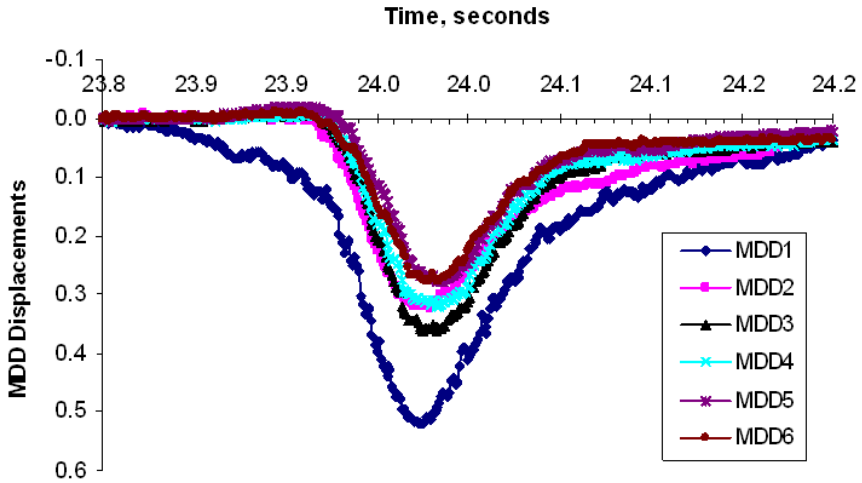

(a)

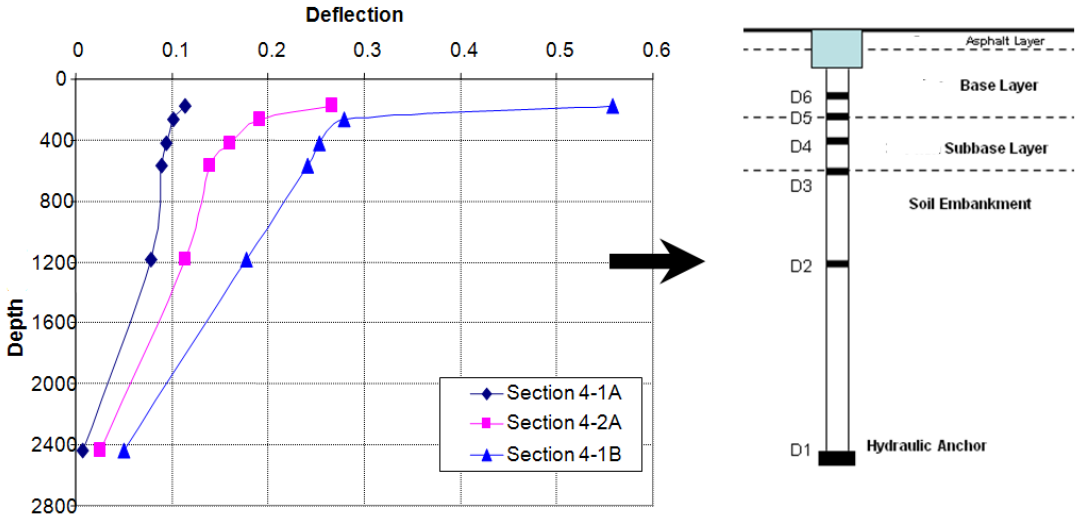

(b)

Figure 15
(a) Typical MDD deflection bowl; (b) typical deflection profiles

The peak deflection profiles can be used to back-calculate the elastic moduli for the pavement layers with a linear elastic multi-layer program *[11]*. However, such deflection profiles sometimes varied significantly due to the combined effects of environmental variation and traffic loading on the elastic characteristics of pavement layers. The typical profile shown in Figure 15(b) indicates that, in general, section 4-1A developed the smallest elastic deformation at all depths among the three sections evaluated, followed by section 4-2A and section 4-1B.

On the other hand, the plastic deformation measured from MDD can be used to calculate the permanent deformation developed at each pavement structural layer. It should be noted that, due to very small surface permanent deformation (or rut depth) observed at the MDD location of section 4-1A, the plastic deformation retrieved from this MDD was fairly small and noisy with the baseline of each of the six MDD potentiometers continuously changing up and down. At the end of 225,000 repetitions, the maximum plastic deformation obtained from the MDD in section 4-1A was about 0.02 in. Generally speaking, negligible permanent deformations have been developed among the pavement layers of section 4-1A below the MDD reference head (4 in. below the surface). Noticeable permanent deformations were observed on both sections 4-2A and 4-1B. Figure 16 depicts the permanent deformation development curves for three pavement layers at sections 4-2A and 4-1B.

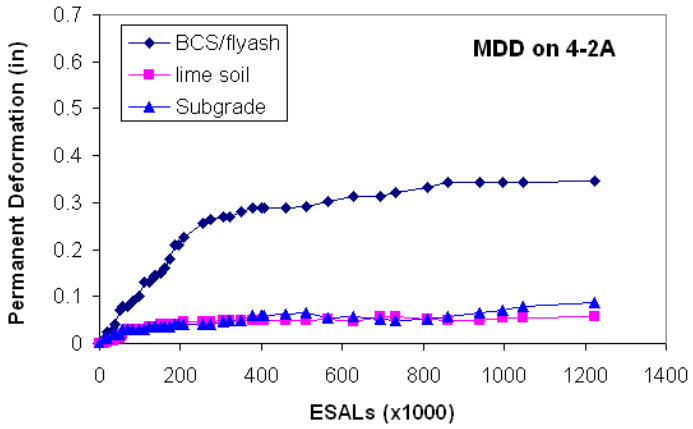

(a)

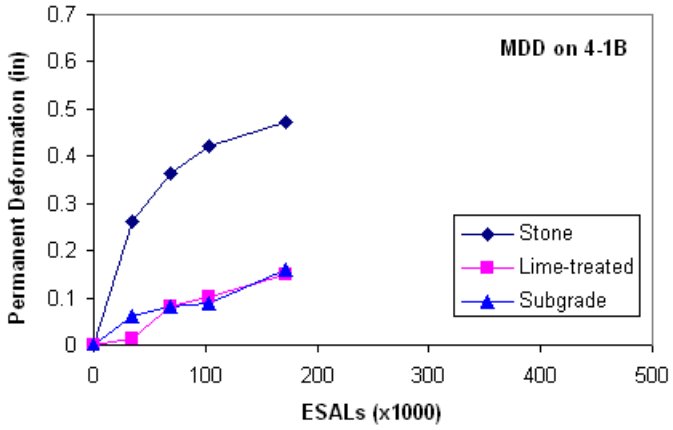

(b)

Figure 16
(a) Plastic deformation at section 4-2A; (b) Plastic deformation at section 4-1B

Figure 16(a) indicates that a significant amount of permanent deformation was developed on the BCS/Flyash layer of section 4-2A, with a similar small amount of permanent deformation developed on both the lime-treated soil and the subgrade. As shown in Figure 16(b), a large amount of permanent deformation was also observed on the base layer (crushed stone) of section 4-1B. The MDD results indicated that the stone layer, lime-soil layer, and subgrade each contributed 70, 15, and 15 percent, respectively, to the total surface rut depth developed in the MDD station. In general, the MDD plastic deformation results appeared to agree well with the vertical compressive stress results described above. The base layers of both sections 4-2A and 4-1B developed large permanent deformation due to receiving higher vertical stress than the bottom layers. However, to achieve a similar permanent deformation, section 4-2A with a fly ash stabilized BCS base required a significantly larger number of load repetitions

than section 4-1B with a stone base (Figure 16). The MDD-measured permanent deformation is very useful in a better understanding of material behavior in a pavement structure. It also can be used in calibrating the rutting model, such as the one used in the newly developed M-E pavement design guide. Additional research of using those MDD measurements is under investigation.

The APT Results

Measured Surface Rut Depths

Figure 17 provides the average rut depth development for the three sections tested. The corresponding ALF load levels at different load repetitions are also provided in the figure. Note that a mechanical-based rut measurement apparatus called "A-Frame" was used in the surface rut depths in this study at eight specified stations under the load area. According to the failure criteria, all three sections were considered as rutting failure (i.e., the average rut depth reached to the 0.5-in. limit at failure). No visible fatigue or alligator cracks were observed on either section 4-1A or 4-2A. However, section 4-1B was observed to develop some medium-severe alligator cracks when its average rut depth reached to 0.5 in.

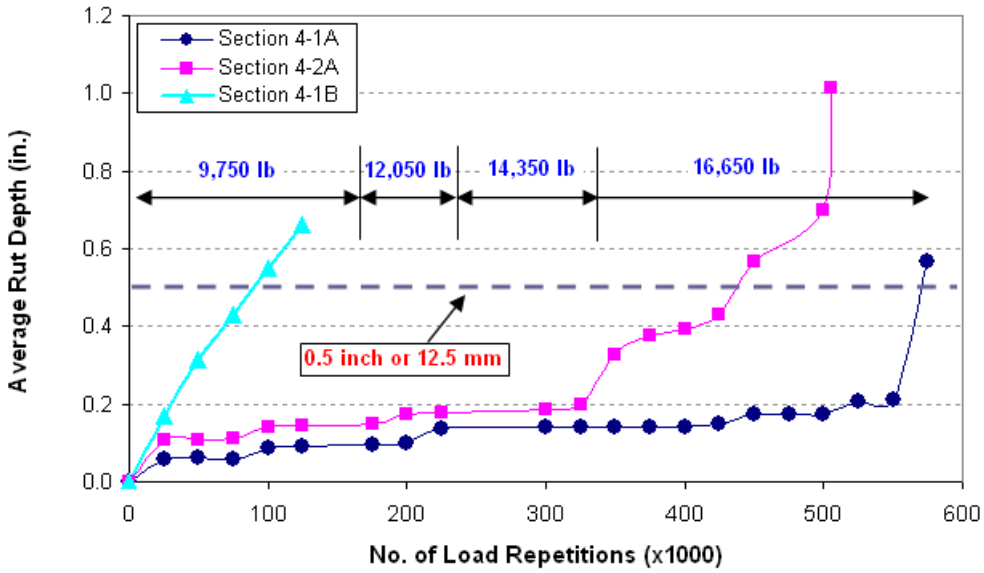

Figure 17
Rut depth development on test sections

As shown in Figure 17, section 4-1A with a BCS/Slag base performed significantly better than other two sections by receiving a total number of 570,000 ALF repetitions before its reaching of the 0.5-in. rutting limit. Next was section 4-2A with a BCS/Fly ash base and 436,000 total repetitions at a rutting failure. The worst performed section was section 4-1B,

whose base was a crushed stone and only lasted 86,000 passes before reaching to an average rut depth of 0.5 in.

Post-Mortem Trenches

Figure 18 shows transverse trench results for the three test sections investigated. Each trench was about 2 ft. wide and 10 ft. long. The measured transverse profiles in Figure 18 indicate that both sections of 4-2A and 4-1B had a base shear flow failure; whereas, section 4-1A failed primarily due to further densification of the BCS/Slag base layer under the load. No visible deformation was observed on the trench below the BCS/Slag layer. The shear failures in sections 4-2A and 4-1B may be partially attributed to the very thin HMA layer used. However, it also indicated insufficient shear strengths provided by those base materials.

Summary on APT Experimental Results

The aforementioned APT results generally indicated that the slag stabilized BCS base in section 4-1A outperformed other two base materials (BCS/Flyash and stone) by a significantly large margin. In terms of cumulative ESALs, when a test section reaches its average rut depth of 0.5 in., the pavement life of section 4-1A (BCS/Slag) would be 3.9 million, followed by section 4- 2A (BCS/Flyash) with 2.3 million, and followed by section 4-1B (crushed stone) with 0.12 million only. The laboratory RLT results shown in Table 9 and Figure 9 also showed that the BCS/Slag had the highest M_r value and lowest permanent deformation as compared to BCS/Flyash and the crushed stone evaluated. The field supporting evidence include the smallest FWD center deflections, negligible permanent deformation at the first 225,000 ALF passes, smallest vertical compressive stresses at two depths, no visible surface cracking, and a longest pavement rutting life. Post-mortem trench results further revealed that, even at the end of a rutting failure, the slag stabilized BCS base in section 4-1A was observed to hold together well as a lean concrete layer. On the other hand, the fly ash stabilized BCS base was also found to perform better than the stone base evaluated. Based on the APT performance results, it is concluded that both a slag stabilized and a fly ash stabilized BCS materials can be served as good candidates in lieu of the crushed stone base in a flexible pavement construction in Louisiana.

(a) Section 4-1A

(b) Section 4-2A

(c) Section 4-1B

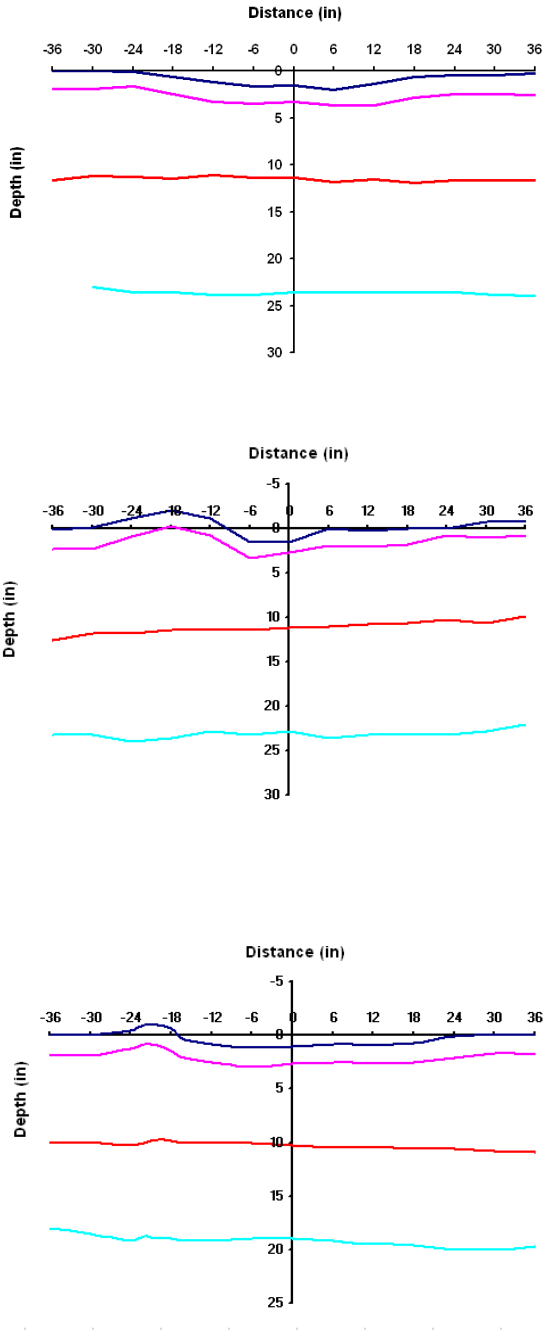

Figure 18
Post-mortem trench results

Permanent Deformation Analysis Using the MEPDG

Figure 19(a) presents the predicted surface rut depths for the three test sections evaluated. In general, the MEPDG software seems to be able to correctly rank the three test sections in terms of their overall performance in rut resistance, that is, section 4-1A performed better than section 4-2A, and section 4-2A was better than section 4-1B. As compared with the average measured rut depths in those three sections [Figures 19(b) - (d)], however, the MEPDG software generally over-predicted the rut depths on sections 4-1A and 4-2A and under-estimated the rut depths in section 4-1B.

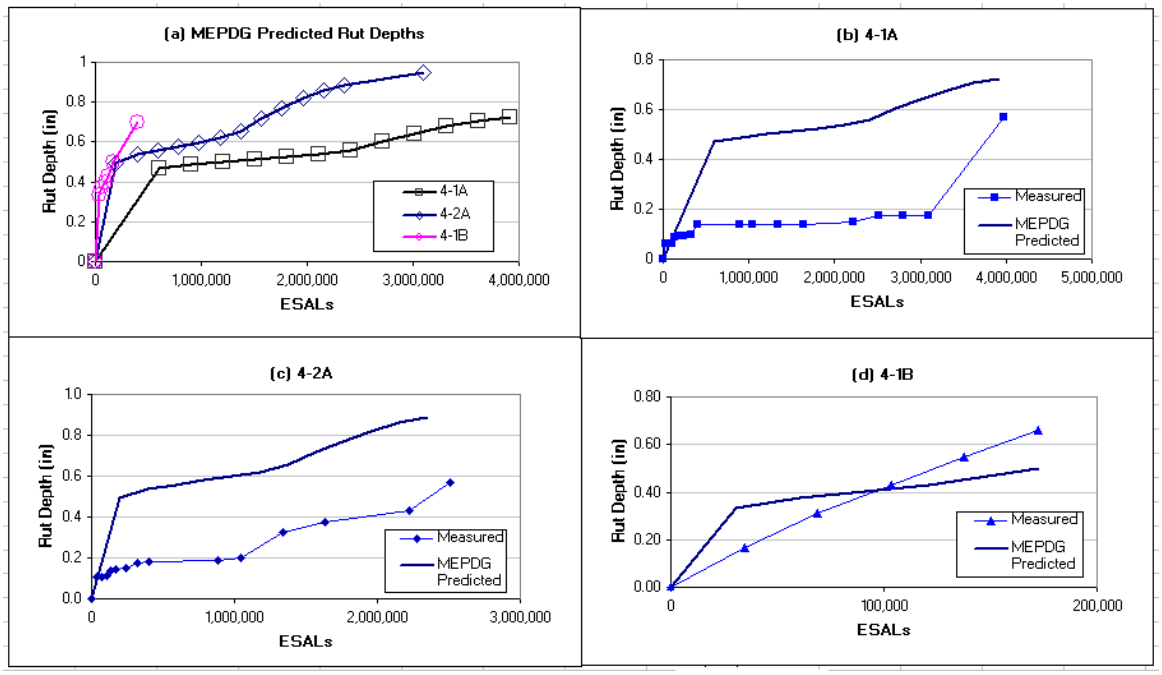

Figure 19
MEPDG predicted rut depths

Further investigation on the output files from the MEPDG analysis revealed that it generally under-estimated the rut depths developed in the base layers, but it over-predicted rutting in the subbase and subgrade layers. Since the rutting potential of chemically stabilized base or subbase materials was not included in the current rutting prediction models used by the MEPDG, therefore, a study on how to predict the rutting on chemically stabilized materials is warranted.

Prediction of Layer Coefficient Values

The structural contribution of pavement materials is quantified by their structural layer coefficients in the 1993 AASHTO pavement design guide. Pavement with a high structural

number (i.e., the summation of layer coefficients multiplied by layer thicknesses) is assumed to have a long pavement structural life.

In order for those tested BCS base materials to be used in a pavement design, a representative design layer coefficient value needs to be provided. To get those design layer coefficient values, the performance results of the six test sections (4-1A, 4-2A, 4-3A, 4-1B, 4-2B, and 4-3B) included in the ALF 4 experiment (as mentioned in the Introduction of this report) were used. The following steps were taken in the determination of layer coefficients for those stabilized materials:

1. The number of ALF load repetitions required for a test section to fail (i.e., meet one of two failure criteria) was considered as its pavement life, which was translated into an ESAL value based on the fourth power law *[5]*.

2. With the known total structural numbers on two control sections (sections 4-1B and 4-2B), a log-linear relationship between pavement lives and the total structural number was constructed.

3. Based on the above relationship, the total structural numbers for sections 4-1A, 4-2A, 4-3A, and 4-3B were backcalculated.

4. Lastly, with the known thicknesses of each test section and layer coefficients for HMA (0.44), lime-soil (0), and cement treated soil (0.06), layer coefficients for stabilized bases were backcalculated from the predicted total structural layer coefficients: BCS/Slag of 0.34 and BCS/Fly ash of 0.29 *[16]*.

The developed log-linear relationship is plotted in Figure 20(a). Note that the six points plotted on the figure represent six test sections outlined in Figure 1. For validation purposes, the backcalculated structural numbers were used into the 1993 AASHTO flexible pavement design equation for predicting the allowable ESAL values on each test section. A subgrade resilient modulus of 12,000 psi was used in the design by considering the contribution from the lime or cement layer to the subgrade. Other design inputs were selected based on a low-volume road design, including the reliability of 95 percent, the standard deviation S_0 of 0.47, and ΔPSI of 1.8. The predicted allowable ESAL values are plotted in Figure 20(b) against the results from this study. The overall prediction was quite good, with the predicted lives on sections 4-1A and 4-2A being slightly lower than the measured ones. This indicates that the predicted structural numbers, if used in a pavement design, will be on the conservative but safe side.

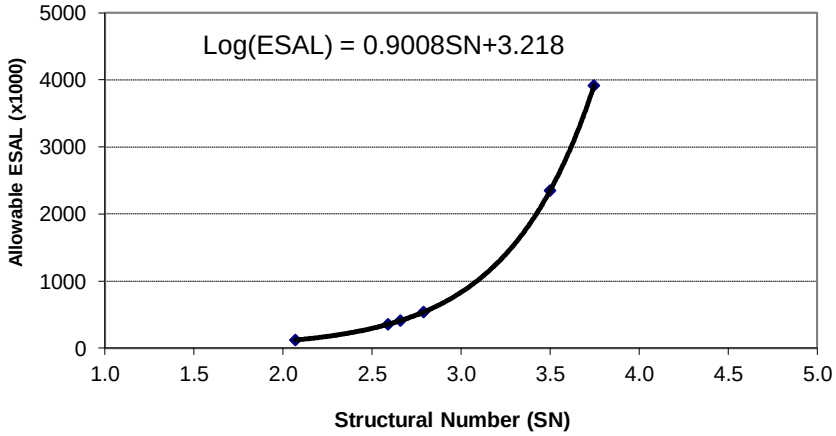

(a)

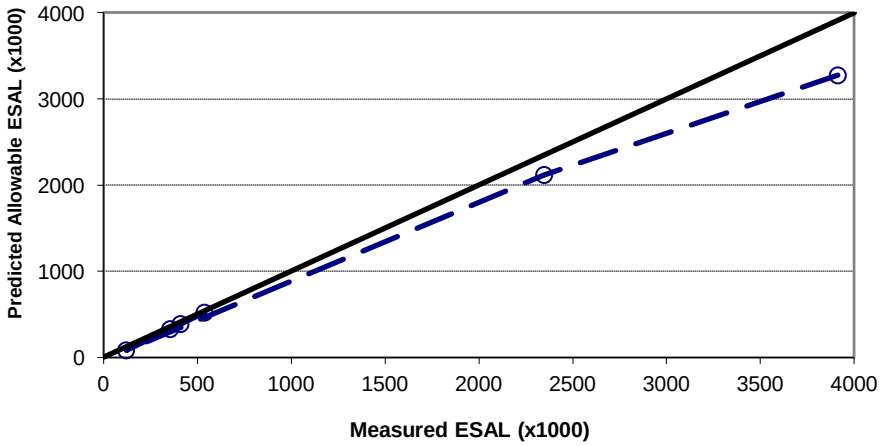

(b)

Figure 20
(a) Log-linear relationship between pavement lives and SN; (b) predicted vs. measured pavement lives

It is interesting to note that, because the AASHTO pavement design equation was derived from the AASHTO road test, this may be the reason why the pavement lives observed in this APT study matched quite well with those predicted from the AASHTO pavement design equation.

Cost/Benefit Analysis

Construction Cost Analysis

To quantify cost benefits from using slag stabilized BCS materials, a construction cost analysis was performed on two pavement structure alternatives. As outlined in Figure 21, Alternative A had the same pavement structure as section 4-1A; whereas, Alternative B used a similar structure as section 4-1B but had a different HMA thickness. The two alternatives were designed to have the same design SN (structural number). According to the 1993 AASHTO design guide, both alternatives should be expected to have the same future performance and pavement lives. The SN value was determined based on layer thicknesses and layer coefficient values *[17]*. A layer coefficient of 0.34 was assigned for a BCS/Slag layer; whereas, the layer coefficients of a new HMA and a crushed stone layers were assumed to be 0.44 and 0.14, respectively. No structural value was assigned to a lime-treated "working table" layer based on engineering judgment. By using those layer coefficients and thickness values showed in Figure 21, both alternative pavement structures would result in a total SN value of 3.77. Such design results indicated that by using a slag-stabilized BCS base in lieu of stone, the thickness of the HMA layer could be significantly reduced (i.e., a 3.8-in. reduction as comparing Alternative A and B, Figure 21).

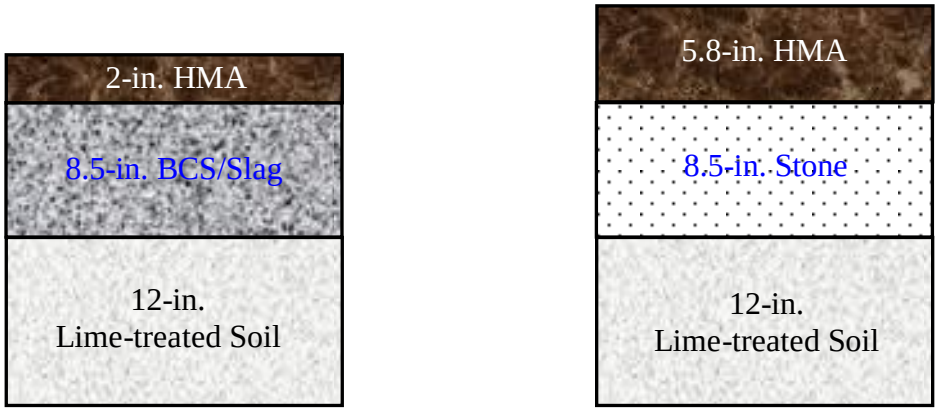

Figure 21
Pavement alternatives used in cost-benefit analysis

The construction costs of two pavement alternatives are listed in Table 15. The unit prices in the table were determined from the construction costs of this APT experiment. The quantities were calculated based on a 13-ft. wide lane for one mile long. As shown in Table 15, the estimated construction costs for Alternatives A and B were $461,853.56 and $547,370.36, respectively. Therefore, by using a slag stabilized BCS base in lieu of a stone base, the

estimated cost benefits would be $85,517 per lane mile. Applying the estimated cost benefits to a typical 2-lane, 10-mile long roadway rehabilitation project, the use of a slag stabilized BCS base in lieu of a stone base can result in a total construction cost savings up to $1,710,340.

Table 15
Initial construction costs

Alternative A			
Materials	Unit Prices ($)	Quantity	Construction Costs($)
2-in. HMA	92.4 per ton	838.9 ton	77,514.36
8.5-in. BCS/Slag	3.5 per ft^2	68,632 ft^2	240,212.00
12-in. Lime-treated Soil	2.1 per ft^2	68,632 ft^2	144,127.20
Total Initial Construction Costs			$461,853.56

Alternative B			
Materials	Unit Prices ($)	Quantity	Construction Costs($)
5.8-in. HMA	92.4 per ton	2432.9 ton	224,799.96
8.5-in. Stone	2.6 per ft^2	68,632 ft^2	178,443.20
12-in. Lime-treated Soil	2.1 per ft^2	68,632 ft^2	144,127.20
Total Initial Construction Costs			$547,370.36

Life-Cycle Cost Analysis (LCCA)

To further demonstrate the benefit of using stabilized BCS materials in lieu of a stone base in pavement construction, an LCCA (life-cycle cost analysis) was performed based on the APT test results in this study. Since a typical flexible pavement structure for a low-volume road in Louisiana consists of a 3.5-in. HMA layer and an 8.5-in. base over a treated soil subgrade, three pavement structure alternatives similar to the corresponding APT test sections were considered in the LCCA with an HMA layer thickness of 3.5 in. instead of 2.0 in., as shown in Figure 22. During the LCCA, the initial annual traffic was assumed to be 200,000 ESALs with an annual growth rate of 2 percent. The 1993 AASHTO pavement design guide's flexible pavement design equation was employed to predict the total ESAL number of each alternative pavement section before a resurfacing maintenance is required for that section, where the design structural number was determined using the layer coefficient values obtained from the APT results, and a difference of 1.5 between the initial design

serviceability index and the design terminal serviceability was allowed. The predicted ESAL numbers for each alternative pavement section was then translated into a pavement performance period in terms of years. At the end of a pavement performance period, a typical resurfacing maintenance activity of milling 2 in. of the existing HMA layer followed by a 4 in. overlay was considered. During a 30-year design life period, resurfacing maintenance was carried out at 23.1-, 14.5-, and 4.8-year intervals in sections of BCS/Slag (Alternative A), BCS/Flyash (Alternative B), and stone (Alternative C), respectively.

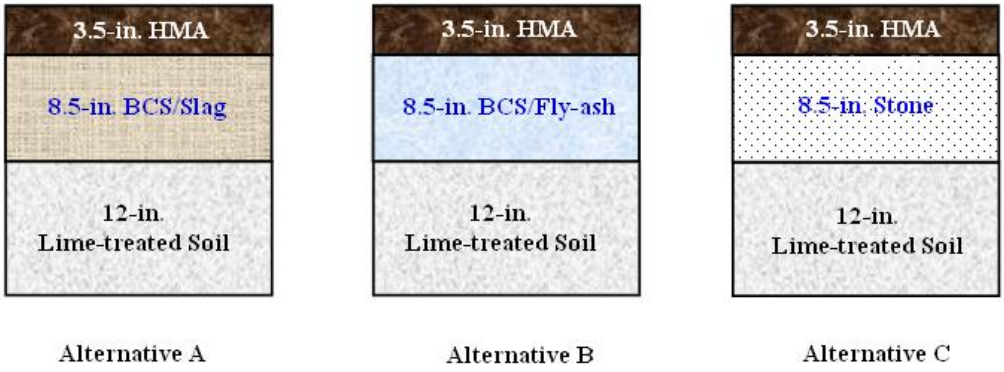

Figure 22
Pavement alternatives used in LCCA

The initial construction costs of three pavement alternatives are listed in Table 16. The unit prices in the table were determined from the construction costs of this APT experiment. The quantities were calculated based on a one-mile long and 13-ft. wide lane. As shown in Table 16, the estimated construction costs for Alternatives A, B, and C were approximately $519,982; $370,365; and $458,214 per lane mile, respectively. Hence, the initial construction cost by using BCS/Slag would be the highest among the three alternatives.

The unit cost for the resurfacing maintenance (2-in. milling and 4-in. overlay) was taken as $51.40 per yd^2. The present worth cost (PWC) was estimated at each scheduled activity of each alternative structure based on a discount rate of 4 percent. The total LCCA costs per lane mile (initial construction cost plus the PWCs in a 30-year period) were then determined to be $649,989 for the BCS/Slag section; $682,071 for the BCS/Flyash section; and $1,629,637 for the stone section. As expected, the BCS/Slag pavement structure showed the lowest total LCCA cost among the three alternatives considered, followed by the BCS/Flyash base and crushed stone base pavement structure. The estimated LCCA PWC costs further indicate that the use of a slag stabilized or a fly ash stabilized BCS bases in lieu of a stone base can potentially result in a LCCA cost savings up to 60 percent and 58 percent per lane mile, respectively.

Table 16
Initial construction costs/lane mile

Alternative A: **BCS/Slag** Materials	Unit Prices ($)	Quantity	Construction Costs($)
3.5-in. HMA	92.4 per ton	1468.0 ton	135,643.20
8.5-in. BCS/Slag	3.5 per ft^2	68,632 ft^2	240,212.00
12-in. Lime-treated Soil	2.1 per ft^2	68,632 ft^2	144,127.20
Total Initial Construction Costs			$519,982.40

Alternative B: **BCS/Flyash** Materials	Unit Prices ($)	Quantity	Construction Costs($)
3.5-in. HMA	92.4 per ton	1468.0 ton	135,643.20
8.5-in. BCS/Fly ash	1.32 per ft^2	68,632 ft^2	90,594.24
12-in. Lime-treated Soil	2.1 per ft^2	68,632 ft^2	144,127.20
Total Initial Construction Costs			$370,364.64

Alternative C: **Stone** Materials	Unit Prices ($)	Quantity	Construction Costs($)
3.5-in. HMA	92.4 per ton	1468.0 ton	135,643.20
8.5-in. Stone	2.6 per ft^2	68,632 ft^2	178,443.20
12-in. Lime-treated Soil	2.1 per ft^2	68,632 ft^2	144,127.20
Total Initial Construction Costs			$458,213.60

CONCLUSIONS

Two cementitiously stabilized BCS test sections–one with a 10 percent by volume slag stabilized BCS base (BCS/Slag) and the other with a 15 percent by volume fly ash stabilized BCS base (BCS/Flyash)–were tested using the ALF wheel load at the Louisiana PRF test site. A control test section built with a typical Class-II crushed limestone base course was also tested. Each test section was instrumented with one MDD and two earth pressure cells for measuring load-induced pavement responses under the ALF wheel load. Surface distress surveys and NDT deflection tests (FWD and Dynaflect) were performed at the end of every 25,000 load repetitions. This accelerated loading experiment was conducted under a natural, unconfined southern Louisiana pavement condition.

The overall APT results indicated that the 10 percent slag stabilized BCS base material outperformed a Class-II limestone base by a significantly large margin. The 15 percent fly ash stabilized BCS base also performed significantly better than the crushed stone base. Based on the overall structural performance and rut-resistance, it is concluded that both the slag and fly ash stabilized BCS materials evaluated in the study should be a good base material candidate in lieu of a crushed stone base for a flexible pavement design in Louisiana.

Some other specific observations and conclusions can also be drawn from this study:

- The APT pavement lives (i.e., the number of ESAL load repetitions before a test section is reached to a 0.5 in. rutting limit) for the three test sections of BCS/Slag, BCS/Flyash and crushed stone were found to be 3.9, 2.3, and 0.1 million ESALs, respectively. Both stabilized BCS test sections had a significant longer pavement life than the crushed stone section evaluated.

- A construction cost analysis demonstrated that the implementation of a slag stabilized BCS base in lieu of a crushed stone base will lead to a thinner asphalt pavement design, which can result in an initial construction cost reduction up to 16 percent. A 30-year life cycle cost analysis based on a typical Louisiana low volume road pavement structure indicated that using an 8.5-in. slag stabilized or an 8.5-in. fly ash stabilized BCS base course in lieu of an 8.5-in. crushed stone base will potentially result in an LCCA cost savings up to 60 percent and 58 percent, respectively, per lane mile.

- The FWD backcalculation results indicated that in-situ modulus of a BCS/Slag layer of 1,190 ksi to 2,730 ksi could be achieved much higher than the modulus of an HMA layer.

- When comparing the predicted and measured pavement responses, it was found that the multi-layer elastic theory generally over-predicted a vertical compressive stress for an unbound layer but under-predicted for bounded base layers used in this study.

- The new MEPDG software version 1.0 was found to generally under-estimate the base rutting but over-predict the rutting for both subbase and subgrade layers.

- MDD results indicated that most of the permanent deformation came from the base layers evaluated. The MDD measured layer permanent deformation is useful in the calibration of the new MEPDG rutting models.

- Based on the APT results, the structural layer coefficients for the BCS/Slag and BCS/Flyash base courses used in this APT study were estimated to be 0.34 and 0.29, respectively. Before implementation of the new MEPDG, those estimated layer coefficient values may be considered for use in the current empirical-based pavement design practice.

- Post-mortem trench results revealed that, even at the end of a rutting failure, the BCS/Slag base performed just like a lean concrete layer inside the pavement without any moisture induced damage issues. In addition, the post-mortem trench results also showed a shear failure initialized inside the BCS/Flyash and stone base layers.

RECOMMENDATIONS

It is recommended that LADOTD begin implementing a 10 percent by volume slag stabilized BCS in lieu of a Class-II crushed stone base course in a flexible pavement design for both medium and high volume roads. A 15 percent by volume fly ash stabilized BCS is also recommended instead of the crushed stone base. It is further recommended that LADOTD use the slag stabilized BCS materials in perpetual flexible pavement design, where a full-depth asphalt concrete layer may be partially replaced by a slag stabilized BCS layer without compromising its long-lasting pavement performance.

ACRONYMS, ABBREVIATIONS, & SYMBOLS

AADTT	Average Annual Daily Truck Traffic
AASHTO	American Association of Highway and Transportation Officials
AC	Asphalt Concrete
ALF	Accelerated Load Facility
APT	Accelerated Pavement Testing
BCS	Blended Calcium Sulfate
COV	Coefficient of Variation
DOT	Department of Transportation
Dynaflect	Dynamic Deflection Determination System
D1	Deflection Measured at Center of FWD Plate
ESAL	Equivalent Single Axle Load
FA	Foamed Asphalt
FWD	Falling Weight Deflectometer
GGBFS	Granulated Ground Blended Furnace Slag
HMA	Hot Mix Asphalt
ITTE	Institute of Transportation and Traffic Engineering
LADOTD	Louisiana Department of Transportation and Development
LCCA	Life Cycle Cost Analysis
LTRC	Louisiana Transportation Research Center
LTPP	Long Term Pavement Performance
MDD	Multi Depth Deflectometer
MEPDG	Mechanistic Empirical Pavement Design Guide
M_r	Resilient Modulus of Subgrade
MTV	Material Transfer Vehicle
NDT	Non-Destructive Testing
PI	Plastic Index
PRF	Pavement Research Facility
PWC	Present Worth Cost
RAP	Reclaimed Asphalt Pavement
RLT	Repeated Load Test
RMS	Root Mean Square
SN	Structural Number
UCS	Unconfined Compressive Strength
WESLEA	Waterways Engineering Station Elastic Layer Analysis Pavement Suite

REFERENCES

1. Zhang, Z., and Tao, M. *Stability of Calcium Sulfate Base Course in a Wet Environment*. LTRC Report No. 419, Baton Rouge, LA., 2006.

2. Tao, M., and Zhang, Z. "Enhanced Performance of Stabilized By-Product Gypsum," *Journal of Materials in Civil Engineering*, Vol. 17, No. 6, ASCE, 2005, pp. 617-623.

3. ASTM D 1557. "Standard Method Tests for Moisture-Density Relations of Soils and Soil Aggregate Mixtures Using 10 Pound Rammer and 18-inch Drop," *Annual Book of ASTM Standards*, Vol. 04.08, pp. 132-141.

4. ASTM D1556-00. "Standard Method Tests for Density and Unit Weight of Soil in Place by the Sand-Cone Method," *Annual Book of ASTM Standards*, Vol. 04.08, pp. 125-131.

5. *Louisiana Standard Specifications for Roads and Bridges*. State of Louisiana, Department of Transportation and Development, Baton Rouge, 2000 Edition.

6. AASHTO T 307. "Determining the Resilient Modulus of Soils and Aggregate Materials," *American Association of State Highway and Transportation Officials*, T 399-07, 2003.

7. Kinchen, R.W., and W.H. Temple. *Asphalt Concrete Overlays of Rigid and Flexible Pavements*. Report No. FHWA/LA-80/147, Louisiana Department of Transportation and Development, 1980.

8. Pierce, L. M., and Mahoney, J. P. "Asphalt Concrete Overlay Design Case Studies." In *Transportation Research Record 1543*, Transportation Research Board, National Research Council, Washington, D.C., 1996, pp. 3-9.

9. *Guide for Mechanistic-Empirical Design of New and Rehabilitated Pavement Structures*, Part 2, Design Inputs, National Cooperative Highway Research Program (NCHRP), Final Report, NCHRP 1-37A, March 2004.

10. Kim, Y.R., Ranjithan, S.R., Troxler, J.D., and Xu, B. *Assessing Pavement Layer Condition Using Deflection Data*. Final Report, NCHRP Project 10-48. North Carolina State University, Raleigh, 2000.

11. Park, S.W., and Fernando, E.G. Sensitivity Analysis of Stress-Depebdent and Plastic Behavior for loading Zoning. *Proceedings of the 5th International Conference on the Bearing Capacity of Roads and Airfields*, Vol. 2, Trondheim, Norway, 1998, pp. 627-636.

12. Lukanen, E.O., Stubstad, R., and Briggs, R. *Temperature Predictions and Adjustment Factors for Asphalt Pavement*. Publication FHWA-RD-98-085, FHWA, 2000.

13. Ullidtz, P., Askegaard, V., and Sjolin, F.O. "Normal Stresses in a Granular Material Under Falling Weight Deflectometer Loading." *Transportation Research Record 1540*,

Transportation Research Board, National Research Council, Washington, D.C., 1996, pp. 24-28.

14. Ullidtz, P. "Deterioration Models for Managing Flexible Pavements," *Transportation Research Record1655*. Transportation Research Board, National Research Council, Washington, D.C., 1999, pp. 31-34.

15. Dunnicliff, J. *Geotechnical Instrumentation for Monitoring Field Performance*, Wiley, New York, 1993.

16. Wu, Z., Zhang, Z., and Morvant, M. "Performance of Various Base/Subbase Materials under Accelerated Loading," CD-ROM, *The 87th Transportation Research Board Annual Meeting*, Transportation Research Board of the National Academies, Washington, D.C., 2008.

17. American Association of State Highway and Transportation Officials (AASHTO). *AASHTO Guide for Design of Pavement Structures*, Washington, D.C., 1993.

APPENDIX

Construction of ALF Experiment No. 4

ALF 4 Experiment Design

Test Section Layout. In ALF Experiment No. 4 (ALF 4), three 13-ft. wide by 215-ft. long flexible pavement test lanes as outlined in Figure 1 were constructed over an existing 5-ft. embankment at LTRC's pavement research facility site in Port Allen, LA. The PRF is a permanent, outdoor, full scale accelerated pavement testing laboratory administrated and operated by LTRC. The purpose of this facility is to test and quantify full-scale pavement performance of various pavement types under accelerated loading using the Accelerated Loading Facility device.

The three lanes were further divided equally into six test sections with different pavement structures. Figures 23 and 24 illustrate cross sections for each test section constructed. In general, each section receives a 2-in. Superpave wearing course mixture placed over the base course. Section 4-1A consists of an 8.5-in. slag stabilized BCS base course over 12 in. of lime treated subbase with 10 percent lime content. Section 4-2A consists of an 8.5-in. fly-ash stabilized BCS base course over a 12-in. lime treated subbase course with 10 percent lime content. Section 4-3A consists of an 8.5-in. foamed asphalt stabilized RAP/reclaimed soil cement blended base course over 12 in. of cement treated subbase with 8 percent cement content. Section 4-1B consists of an 8.5-in. stone base course over 12 in. of lime treated subbase with 10 percent lime content. Section 4-2B consists of an 8.5-in. stone base course over 12 in. of cement treated subbase with 8 percent cement content. Section 4-3B consists of an 8.5-in. foamed asphalt stabilized RAP base course over 12 in. of cement treated subbase with 8 percent cement content.

The selection of a 2-in. thick asphalt layer used in test sections was due to the consideration that this experiment was to investigate the performance of bases and subgrade layers. Also included in the design was the installation of a perforated drain pipe system located at one edge of each test lane (Figures 23 and 24). A soaker type hose was inserted into the drain pipes to be able to add water to the embankment as required.

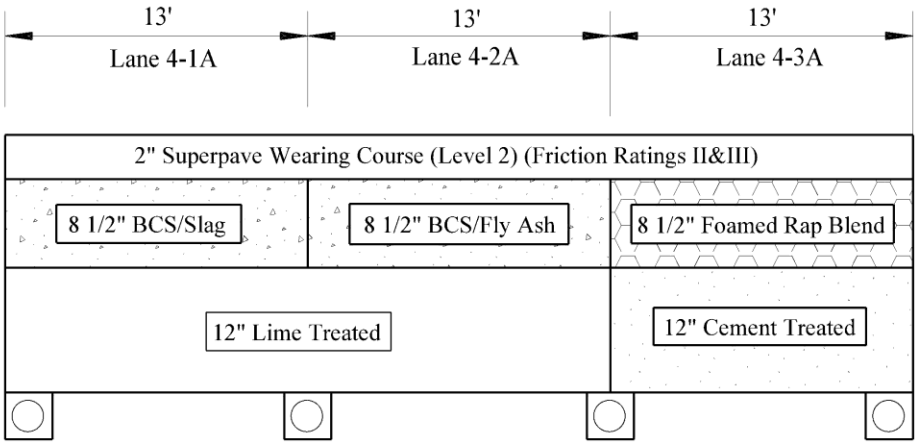

TYPICAL SECTION

STATION 0+00 THRU 1+07.5

Figure 23
Cross section of "A" test lanes

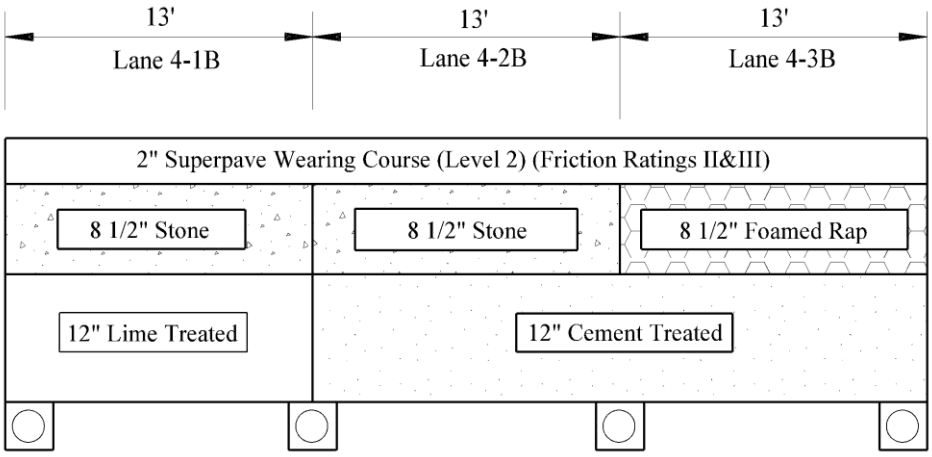

Drain pipe Drain pipe

TYPICAL SECTION

STATION 1+07.5 THRU 2+15

Figure 24
Cross section of "B" test lanes

Table 17
Gradation and specification requirements for Class-II stone base

U.S. Sieve	Specification	Percent Passing
1½ in.	100	100
1 in.	90~100	97
¾ in.	70~100	88
½ in		74
3/8 in		67
# 4	35~65	50
# 8		36
# 16		26
# 30		20
# 40	12~32	n/a
# 50		15
#200	5~12	11

Construction of Test Sections

The contract for construction was awarded to F.G. Sullivan, Jr. Contracting of Baton Rouge, Louisiana, for $265,426. Construction of the three test lanes began in November 2004 and was completed in March 2005. Normal construction practices were followed so that the project would be as representative as possible of actual highway practices, all in accordance with *Louisiana Standard Specifications for Roads and Bridges, 2000 [5]*.

Embankment Construction. Construction of the new test lanes began by removing one existing test lane and the shoulder used in a previous experiment. An ALTEC RW18 vemeer type joint cutter was used to cut a joint along the edges of the test lanes to be removed. The contractor used a Roadtech RX-60 roto-milling machine to reclaim the existing asphalt pavement. This RAP material was stockpiled near the construction area to be used in the foamed asphalt test sections. The contractor also removed the shoulder and base materials using a Hitachi EX200-LC track hoe and bulldozer. Embankment material was excavated from an area just past the original shoulder and placed on the test lanes to established grade for subbase treatment. The material was spread, leveled, and compacted prior to treatment.

Perforated Drainpipe System Installation. The contractor began installing the 4-in. perforated drainpipe system by removing a 9-in. wide trench in the existing embankment using a 9-in. wide Ditchwitch trencher. An approved geotextile fabric was placed along the sides and bottom to line the trench. The trench was then partially back filled with approved

pea gravel. Table 18 shows the gradation of the pea gravel. The 4-in. schedule 35 perforated PVC pipe was then placed and subsequently the trench was backfilled with the remaining pea gravel. The fabric was draped over the top of the trench and secured using "U" shaped spikes. Prior to covering the drain, a soaker type hose was inserted throughout the length of each drain pipe to allow moistening of the embankment and subbase as required in the experiment.

Table 18
Pea gravel gradation for drainage system

Material		Pea Gravel		
Sieve Size	Weight, lb.	%	% Coarse	% Passing
1½"	0	0.00	0.00	100.00
1"	0	0.00	0.00	100.00
¾"	0	0.00	0.00	100.00
½"	0	0.00	0.00	100.00
3/8"	40.2	2.10	2.10	97.90
No. 4	1487.4	76.75	78.85	21.25
No. 8	347.7	18.15	99.90	2.10
No. 10	0	0.00	97.90	2.10
No. 16	27.8	1.45	99.35	0.65
No. 30	0	0.00	99.35	0.65
No. 40	0	0.00	99.35	0.65
No. 50	0	0.00	99.35	0.65
No. 80	0	0.00	99.35	0.65
No. 200	7.9	0.41	99.77	0.23
Pan	1.9			
Dec	2.6			
Total	1915.5	+ 4 Mat.	1527.6 lb.	
Initial	1912.9	Cr. Mat.	0.0	
a/wash	1910.3	% Cr.	0.0	

Prior to the construction of the subbase, PRF personnel began placing moisture gages and pressure cell instrumentation just below the surface of the embankment.

Subbase Construction. Construction of the new test lanes continued with lime or cement treatment for each specified section. Lime was spread evenly on sections 4-1A, 4-1B, and 4-2A at a rate of 10 percent by volume. A total of 7.34 tons was distributed over the three test sections. Cement was then spread evenly on sections 4-2B, 4-3A, and 4-3B at a rate of 8 percent by volume. A total of 15.8 tons of cement was spread. A Caterpillar SS 250 stabilizer was used to process both the lime treatment and the cement treatment of the

subbase at the plan depth of 12 in. Initial compaction was accomplished by the Bomag sheep foot roller, followed by a Hyster steel roller.

Final grade was accomplished using a Natalis motor grader followed by the multi-wheel rubber tire roller. Tables 19 and 20 present the nuclear density and moisture content results for the lime-treated and cement-treated subbases, respectively.

A Troxler Nuclear Density gauge was used in the measurement. In general, the average field Proctor density and moisture content for the lime-treated subbase were 98.7 and 17.8 percent, respectively; whereas, for the cement treated subbase, the two measurements were 93.2 and 17.9 percent, respectively.

Table 19
Nuclear density values for lime treated subbase

Lane No. (Station)	Test #	Dry Weight Density	Wet Weight Density	Moisture Content, %	Density, % Proctor
4-1A (0+40)	1	99.8	117.0	17.2	97.8
	2	99.8	116.7	16.9	97.8
	3	99.6	117.5	17.9	97.6
Average Proctor					97.7
4-2A (0+35)	1	98.4	117.5	19.5	96.4
	2	98.9	118.5	19.8	96.9
	3	98.0	117.4	19.7	96.0
Average Proctor					96.4
4-1B (1+40)	1	102.0	119.7	17.4	99.9
	2	102.6	118.8	15.8	100.5
	3	102.0	118.3	16.0	99.9
Average Proctor					100.1

Table 20
Nuclear density values for cemented treated subbase

Lane No.	Test #	Dry Weight Density	Wet Weight Density	Moisture Content, %	Density, % Proctor
4-3A (0+35)	1	92.8	109.8	18.3	89.9
	2	92.8	110.0	18.5	88.9
	3	91.0	109.2	20.0	88.2
Average Proctor					89.0
4-2B (1+60)	1	98.1	115.6	17.5	95.1
	2	98.2	115.4	17.2	95.2
	3	98.3	115.9	17.6	95.3
Average Proctor					95.2
4-3B (1+40)	1	98.2	115.5	17.3	95.2
	2	98.2	115.7	17.5	95.2
	3	98.3	115.9	17.6	95.3
Average Proctor					95.2

Base Construction. The crushed stone was placed on sections 4-1B and 4-2B and spread with a Case 850C Bulldozer to a depth of 8½ in. Grading was accomplished using a Caterpillar motor grader and compaction was achieved using a vibratory steel roller. Water was used to aid in the compaction effort and to achieve proper moisture content. The optimum dry density for the stone was 149.4 lb/ft^3 at 6.3 percent moisture content and the actual field average result was 144.8 lb/ft^3 at 4.0 percent (see Table 21). MC-250 cutback asphalt was used to prime the stone base with a measured 0.25 gallons per square yard.

RAP material was placed in dump trucks with a track hoe and then spread on sections 4-3A and 4-3B to their proper thickness. A stockpile of reclaimed soil cement was then placed on section 4-3A for blending with an addition of 1.5 percent lime. Also, a 1 precent cement was added into the RAP materials of 4-3B prior to mixing with foamed asphalt. Wirtgen WR 2500 S mixing machine from McAsphalt Engineering Services was used to add and blend the foamed asphalt treated bases. Foamed asphalt was achieved by injecting a predetermined amount of cold water into hot asphalt (PG 58-22 grade binder) in the mixing chamber of Wirtgen WR 2500 S. A NYNAPAC CA15 steel roller was used to compact the mixture. Final grading was accomplished using the Caterpillar motor grader. A multi wheel rubber tire roller was used to complete the compaction effort. The nuclear density results for these two test sections are also reported in Table 21.

Table 21
Nuclear density values for base courses

Lane No.	Test #	Dry Weight Density	Wet Weight Density	Moisture Content, %	Density, % Proctor
4-1A (0+60)	1	94.7	122.2	29.1	87.0
	2	92.4	121.0	30.9	85.0
	3	95.4	123.5	29.4	87.7
				Average Proctor	86.6
4-2A (0+60)	1	96.2	122.8	27.6	81.0
	2	94.9	122.4	27.5	79.9
	3	95.8	122.5	26.7	80.7
				Average Proctor	80.5
4-3A (0+60)	1	106.6	126.2	18.4	85.0
	2	106.2	125.8	18.5	84.7
	3	105.5	126.3	19.8	84.1
				Average Proctor	84.6
4-1B (1+80)	1	143.6	149.5	4.1	96.1
	2	145.0	150.4	3.7	97.1
	3	144.9	150.8	4.0	97.0
				Average Proctor	96.7
4-2B (1+80)	1	147.8	154.2	4.4	98.9
	2	144.1	150.4	4.4	96.4
	3	143.1	148.6	3.8	95.8
				Average Proctor	97.0
4-3B (1+80)	1	107.0	124.6	16.4	85.2
	2	109.4	126.7	15.8	87.2
	3	109.8	127.4	16.0	87.6
				Average Proctor	86.7

A BCS (Blended Calcium Sulfate) material was delivered and placed using a Case 850C Bulldozer at the required depth of 8½ in. for sections 4-1A and 4-2A. A GGBFS (Ground Granulated Blast Furnace Slag) was placed on section 4-1A at a rate of 10 percent by volume and blended using a Caterpillar SS 250 stabilizer. Fly ash was placed on Section 4-2A at a rate of 15 percent by volume and blended using a Caterpillar SS 250 stabilizer. Each section was compacted using a multi-wheel rubber-tire roller and final grade established using a Caterpillar motor grader.

HMA Placement. The HMA mixtures were transported from the contractor's (Sullivan) plant located approximately 8 miles north of the Pavement Research Facility for the HMA placement. A conventional paver was used to place a 2-in. HMA layer on the top

of all test lanes. The paver accepted truck-loaded mixtures directly into its receiving hopper, as sufficient distance was not available to incorporate a Material Transfer Vehicle (MTV) that is required on all paving projects in Louisiana. After placement of the HMA, an Ingersoll-Rand DD90 vibratory steel roller followed by a Bomag BW-12 pneumatic wheeled roller was used to compact the HMA mixtures. Surface density measurements were obtained using a Troxler nuclear density device to help establish the rolling pattern. The rolling pattern established was two vibratory steel roller passes, two static steel roller passes, and two pneumatic roller passes for each test lane.

The final grade's elevations along each centerline were measured at 10-ft. intervals before and after the HMA placement. As presented in Table 22, the elevation difference at each station represents the constructed thicknesses of the HMA layers along the centerlines.

Table 22
Measured HMA layer thickness

Station	HMA Thickness (inches)		
	Lane 4-1	Lane 4-2	Lane 4-3
0+00	1.3	2.0	2.0
0+10	1.7	1.2	1.7
0+20	1.4	1.3	1.7
0+30	1.4	1.2	1.8
0+40	1.0	1.8	2.0
0+50	1.9	1.8	1.8
0+60	1.9	1.6	1.7
0+70	2.4	1.4	1.7
0+80	2.4	1.7	1.9
0+90	2.3	1.8	1.9
1+00	2.0	1.6	2.0
1+10	1.7	1.8	1.9
1+20	1.8	1.2	1.7
1+30	1.4	1.2	1.6
1+40	1.0	2.0	1.3
1+50	1.3	1.4	1.7
1+60	1.6	1.4	2.0
1+70	1.4	1.2	1.9
1+80	1.1	1.1	1.9
1+90	1.4	1.4	2.0
2+00	1.6	2.0	2.0
2+10	1.8	2.3	2.2
2+15	1.7	1.4	1.6

In addition, four 6-in. cores were cut along the centerline with a 2.5-ft. left offset at each test section and then sent to the LTRC materials laboratory for air voids and thickness measurements. Table 23 presents the laboratory measurements for these HMA cores.

Table 23
Measured air voids and thickness for HMA cores

4-1A	Air Voids (%)	Thickness (in.)	4-2A	Air Voids (%)	Thickness (in.)	4-3A	Air Voids (%)	Thickness (in.)
0+13	8.6	1.74	0+13	9.7	1.59	0+13	6.6	1.84
0+36	7.2	1.57	0+36	12.3	1.73	0+36	6.9	1.98
0+60	7.8	1.95	0+60	8.8	1.67	0+60	12.2	1.54
0+96	4.7	2.14	0+96	6.3	1.91	0+96	5.8	1.94
Ave.	**7.1**	**1.9**	**Ave.**	**9.3**	**1.7**	**Ave.**	**7.9**	**1.7**
4-1B	Air Voids (%)	Thickness (in.)	4-2B	Air Voids (%)	Thickness (in.)	4-3B	Air Voids (%)	Thickness (in.)
1+18	6.5	2.0	1+18	7.3	1.56	1+18	5.3	1.92
1+40	6.2	1.8	1+40	8.4	1.60	1+40	5.7	1.66
1+78	6.5	1.8	1+78	6.1	1.84	1+78	4.0	2.17
2+02	5.4	2.1	2+02	7.7	2.59	2+02	7.1	1.94
Ave.	**6.2**	**1.9**	**Ave.**	**7.4**	**1.9**	**Ave.**	**5.5**	**1.9**

The installation of MDDs (multi depth deflectometers) was performed on top of finished asphalt surfaces after the construction. A professional staff from the manufacture company was sent to the site for the six MDD installations. In this study, one MDD contains six deformation sensors, each installed at a distance from the surface of 7 in., 10.5 in., 16.5 in., 22.5 in., 46.5 in. and 96 in., respectively (see Figure 2).

Field Testing. During the construction, a suite of in-situ tests was performed on top of each finished pavement layer. Those tests include DCP, FWD, and Dynaflect.

DCP

The DCP (dynamic cone penetrometer) consists of a 60-degree cone connected to a 5/8-in. diameter steel rod, which is advanced into a material by repeatedly dropping a 17.67-lb. hammer onto a fixed anvil located on the rod. Penetration measurements are recorded with each drop and the data indicates material strength and layer changes. The DCP is a useful tool that can be used on many different pavement layers, except concrete and asphalt pavement layers. If stiff layers prevent the advancement of the DCP, a hammer drill is used

to advance to the next lower pavement layer. The DCP can extend about 3-ft. below the bottom of the cored/drilled pavement surface.

The results of a DCP test are used to calculate an average millimeter per blow (mm/blow) for a particular constructed layer. In this method of evaluation, the lower the average mm/blow, the stiffer or stronger the material. In contrast, the higher the average mm/blow, the weaker the material. For example, if the material is extremely stiff and the DCP will not penetrate a layer, 0 in. would represent refusal and no penetration by the cone. In soft material, the DCP can advance several mm/cm with a single blow.

Falling Weight Deflectometer

A Dynatest 8002 FWD was used in this study with nine sensors spaced at 0 in., 8 in., 12 in., 18 in., 24 in., 36 in., 48 in., 60 in., and 72 in. from the center of the load plate. Since FWD loads can be varied by changing the height of a dropping weight, different load levels were chosen for testing on different pavement surfaces. Specifically, four load levels of 1,500, 2,400, 3,000, and 4,000 lb. were used on the top of subbase and base courses; whereas, three load levels of 9,000, 12,000, and 16,000 lb. were selected for testing on HMA surface course.

Dynaflect

The Dynamic Deflection Determination System (Dynaflect) is a trailer mounted device that induces a dynamic load on the pavement and measures the resulting deflections by using five geophones spaced under the trailer at approximately 1-ft. intervals from the application of the load. The pavement is subjected to 1,000 lb. of dynamic load at a frequency of 8 Hz. The Dynaflect measured deflections can be used to estimate the existing pavement structural number and subgrade modulus based on a Pavement Evaluation Chart developed by Kinchen and Temple *[7]*.

Field Test Results

Subgrade Moisture Content – Prior to Construction. As mentioned earlier, moisture sensors were placed within the subgrade to monitor the subgrade area below the treated subbase (lime or cement treatment). Samples were collected during the installation for moisture contents. Table 24 presents the moisture content results. These moisture contents were used to calibrate the moisture sensors placed within the subgrade. The measured moisture contents for the embankment soil ranged from 18.0 to 24.2 percent with an overall average of 20.5 percent, which is about 2 percent higher than the optimum moisture content of 18.5 percent for this soil as showed in Table 4.

Table 24
Moisture content measurement for embankment subgrade

Sample ID	Moisture, %		Sample ID	Moisture, %
4-1B 01+57	20.5		4-1A 00+51	18.0
4-1B 01+54	18.2		4-1A 00+49	18.6
4-1B 01+51	NA		4-1A 00+45	18.9
4-2B 01+57	20.5		4-2A 00+51	23.4
4-2B 01+54	20.7		4-2A 00+48	22.1
4-2B 01+51	20.3		4-2A 00+55	24.2
4-3B 01+57	19.1		4-3A 00+51	20.6
4-3B 01+54	20.0		4-3A 00+48	22.0
4-3B 01+51	18.7		4-3A 00+45	22.7

Treated Subbase Moisture Content – Prior to Stabilization. One objective during the field construction was to treat the subbase soil material in a "wet" condition. To accomplish this objective, the motor patrol passed over the subbase soil prior to the placement and spreading of the additive (lime or cement). The purpose of this pass was to prepare the soil by mixing in moisture. Moisture samples were collected from the sections after the motor patrol passed. Atterberg limits were also conducted on the collected samples. The results are presented in Table 25. Test results indicate that the average moisture contents for lime treated sections (4-1A, 4-2A, and 4-1B) and cement sections (4-3A, 4-2B, and 4-3B) were 17.7 and 14.2 percent, respectively. The plasticity index (PI) ranged from 2 to 10 on both treatment sections. Overall, the untreated subbase soil had a PI value less than or equal to 10. According to the UNO study, this soil should be considered to have a high pumping potential and will become unstable with increased moisture and traffic load *[2]*. Therefore, cement treatment of this soil would provide greater performance benefits than lime treatment in wet conditions.

Table 25
Soil properties of wet subgrade

Station	Section	Moisture Content %	Liquid Limit %	Plasticity Index %		Station	Section	Moisture Content %	Liquid Limit %	Plasticity Index %
1+39	4-1B	21.9	NON-PLASTIC			0+30	4-1A	18.3	31	8
1+50	4-1B	18.2	30	2		0+60	4-1A	19.5	33	7
1+80	4-1B	18.8	30	2		0+80	4-1A	22.2	30	3
1+39	4-2B	11.5	34	3		0+10	4-2A	14.5	33	7
1+60	4-2B	14.5	34	2		0+30	4-2A	11.6	33	6
1+80	4-2B	12.6	34	2		0+60	4-2A	16.1	38	10
						0+80	4-2A	15.7	32	2
1+39	4-3B	14	37	5		0+30	4-3A	15.3	36	8
1+60	4-3B	13.6	36	5		0+60	4-3A	16.7	38	10
1+80	4-3B	14	34	2		0+80	4-3A	15.5	39	9

Density, Moisture Content, and Thickness Measurements during Construction. Table 26 presents the summary results of nuclear density measurements obtained on top of different treated soil layers during the construction. As shown in Table 26, the average densities on the lime-treated and cement-treated layers were 98.1 percent and 93.1 percent, respectively, and the corresponding average in situ moisture contents were 17.8 percent and 17.9 percent.

Table 26
Summary of density measurements on treated soil layers

Section ID	Dry Weight Density (pcf)	Wet Weight Density (pcf)	**Moisture Content, %**	**Density, % Proctor**
	Lime Treated Soil Layers			
4-1A	99.7	117.1	17.3	97.7
4-2A	98.4	117.8	19.7	96.4
4-1B	102.2	118.9	16.4	100.1
			Average	**17.8**	**98.1**
			Standard Deviation	**1.7**	**1.9**
Section ID	**Cement Treated Soil Layers**			
4-3A	92.2	109.7	18.9	89.0
4-2B	98.2	115.6	17.4	95.2
4-3B	98.2	115.7	17.5	95.2
			Average	**17.9**	**93.1**
			Standard Deviation	**0.9**	**3.6**

Table 27 presents the summary density measurement obtained on various base materials during the construction. As shown in Table 27, both stone layers (in sections 4-1B and 4-2B) received an in-situ density value greater than 95 percent. However, the four chemically stabilized base materials (BCS/Slag, BCS/Flyash, and two foamed asphalt treated RAP materials) were found to be constructed with lower density values ranged from 80.5 percent to 86.7 percent. High moisture contents could have resulted in initial low density values for the two stabilized BCS layers; whereas, the high design air voids matched with low density values found in the two foamed asphalt base materials, Table 27.

Table 27
Summary of density measurements on base layers

Section ID Base Type	Dry Weight Density (pcf)	Wet Weight Density (pcf)	**Moisture Content, %**	**Density, % Proctor**
4-1A BCS/Slag	94.2	122.2	**29.8**	**86.6**
4-2A BCS/Flyash	95.6	122.6	**27.3**	**80.5**
4-3A FA(50%RAP)	106.1	126.1	**18.9**	**84.6**
4-1B Stone	144.5	150.2	**3.9**	**96.7**
4-2B Stone	145.0	151.1	**4.2**	**97.0**
4-3B FA(100%RAP)	108.7	126.2	**16.1**	**86.7**

Table 28 presents the average HMA thicknesses and air voids variations on the six test sections constructed. As shown in Table 28, based on measured results of HMA cores, the average air voids of the as-built HMA layers is 7.2 percent, with a range varied from 5.5 percent to 9.3 percent among sections. The highest air voids was received on section 4-2A, while the lowest air voids was on section 4-3B. On the other hand, the HMA core thicknesses varied from 1.7 in. to 1.9 in. with an average value of 1.8 in. Note that the field cores were cut 2.5-ft. left to centerline at each test section, and four cores were taken from each section. Based on the centerline survey results (Table 22 and Table 28), the average as-built HMA thicknesses along the centerline varied from 1.5 in. to 1.8 in. among test sections when the entire section length was considered. The overall HMA thickness value is averaged to be 1.7

in. However, on the future ALF loading areas (Stations 0+40 to 0+70 on "A" sections and Stations 1+40 to 1+70 on "B" sections), the as-built HMA thicknesses varied from 1.3 in. to 1.8 in., with an overall average value of 1.6 in. The thinnest section constructed under the ALF loading area was section 4-1B, followed by section 4-2B. Both sections have a stone base course. Since the design HMA thickness is 2 in. for all six test sections, future performance on these sections could be adversely affected by thin HMA thicknesses. In addition, it was observed that the largest thickness variation under the ALF loading area was on section 4-1A with an average value of 1.8 in. and a standard deviation of 0.6 in., Table 28. In general, satisfactory field compaction was achieved on the HMA layers. However, the overall as-built HMA thickness was found to be slightly thinner than the design.

Table 28
Summary of as-built HMA thicknesses and air voids

Section ID	Data from Field Cores				Thicknesses (in.) from Centerline Survey			
	Air Voids		Thickness (in.)		Entire Section based		Loading Area based	
	Average	STD	Average	STD	Average	STD	Average	STD
4-1A	7.1	0.2	1.9	0.2	1.8	0.5	1.8	0.6
4-2A	9.3	2.5	1.7	0.1	1.6	0.3	1.7	0.2
4-3A	7.9	2.9	1.7	0.2	1.8	0.1	1.8	0.1
4-1B	6.2	0.5	1.9	0.2	1.5	0.3	1.3	0.3
4-2B	7.4	1.0	1.9	0.5	1.5	0.4	1.5	0.3
4-3B	5.5	1.3	1.9	0.2	1.8	0.2	1.7	0.3
Average	**7.2**		**1.8**		**1.7**		**1.6**	

DCP Tests on Subgrade and Treated Subbase. DCP testing began shortly after the treated subbase compaction was completed with the first event on November 23, 2004. Subsequent tests were conducted on a weekly basis for six weeks. The DCP results from each individual location are listed in Tables 29 and 30. Table 29 covers sections where lime treatment was used. Results of cement treatment test sections are presented in Table 30. In each table, an average value was calculated for the three test locations, so a single mm/blow value could represent each section. Thus, the 19 locations were summarized into seven sections (lime sections: raw BCS, BCS w/slag, stone, and BCS w/flyash; cement sections: stone and two foamed asphalts).

Table 29
DCP results (mm/blow) for lime-treated sections

		RAW BCS	BCS W/ Slag				Stone				BCS W/ Flyash			
	Section	4-2A	4-1A				4-1B				4-2A			
Date	Station	0+10	0+30	0+55	0+80	**Average**	1+40	1+58	1+80	**Average**	0+30	0+55	0+80	**Average**
30-Nov	Base	11.4	11.7	14.1	14.6	**13.5**	12.6	10.7	9.9	**11.1**	18.5	12.8	16.1	**15.8**
2-Dec	Base		9.1	7.3	7.4	**7.9**					13.0	11.9	10.6	**11.8**
7-Dec	Base		3.1	2.6	2.6	**2.8**	6.3	5.6	5.2	**5.7**	8.5	7.4	6.7	**7.5**
14-Dec	Base	14.1	1.2	1.2	1.0	**1.1**	6.0	3.5	4.4	**4.6**	5.6	5.6	5.4	**5.5**
21-Dec	Base	4.9	0.6	0.4	0.4	**0.5**	3.2	2.0	2.7	**2.7**	4.5	3.8	3.2	**3.8**
4-Feb	Base	4.5	0.3	0.2	0.2	**0.3**	7.2	3.4	1.1	**3.9**	1.8	1.8	1.6	**1.8**
23-Nov	Subbase	36.0	28.9	30.1	32.8	**30.6**	26.8	22.7	31.0	**26.8**	46.7	31.5	33.9	**37.3**
30-Nov	Subbase	13.5	12.7	13.6	13.0	**13.1**	13.7	11.7	11.7	**12.4**	28.5	13.2	12.1	**17.9**
2-Dec	Subbase		10.6	9.6	10.6	**10.3**					11.5	9.8	9.1	**10.1**
7-Dec	Subbase		12.0	10.5	8.9	**10.5**	17.6	11.4	11.8	**13.6**	10.6	10.5	12.2	**11.1**
14-Dec	Subbase	10.1	9.3	9.7	10.1	**9.7**	21.1	13.1	10.7	**15.0**	10.0	9.1	9.5	**9.5**
21-Dec	Subbase	12.6	10.4	NA	9.6	**10.0**	16.8	11.8	12.5	**13.7**	10.7	10.2	8.5	**9.8**
4-Feb	Subbase	10.9	14.3	10.8	10.5	**11.9**	13.6	13.1	1.9	**9.6**	7.0	9.0	8.0	**8.0**
23-Nov	Subgrade	23.6	19.9	33.3	32.6	**28.6**	30.6	34.1	22.4	**29.1**	27.9	41.6	40.0	**36.5**
30-Nov	Subgrade	17.5	17.8	28.5	31.1	**25.8**	32.6	52.2	32.4	**39.1**	25.6	28.7	23.9	**26.1**
7-Dec	Subgrade		17.0	31.3	18.1	**22.1**	28.4	29.7	29.5	**29.2**	16.7	22.5	32.0	**23.7**
14-Dec	Subgrade	13.8	19.8	22.8	24.7	**22.4**	31.8	31.5	27.3	**30.2**	14.0	28.2	25.3	**22.5**
21-Dec	Subgrade	23.2	15.7	NA	23.2	**19.4**	35.2	23.3	17.3	**25.3**	17.2	32.3	28.9	**26.1**
4-Feb	Subgrade	15.5	22.1	29.0	14.9	**22.0**	16.6	25.4	12.1	**18.0**	18.1	28.7	24.6	**23.8**

Table 30
DCP results (mm/blow) for cement-treated sections

		Foamed Asphalt (50%RAP+50%Soil Cement)				Stone				Foamed Asphalt (100% RAP)			
Date	Section	4-3A				4-2B				4-3B			
	Station	0+30	0+55	0+80	**Average**	1+40	1+58	1+80	**Average**	1+40	1+58	1+80	**Average**
30-Nov	Base	11.9	16.0	16.8	**14.9**	9.5	9.7	7.9	**9.0**	9.1	12.0	14.2	**11.8**
2-Dec	Base												
7-Dec	Base	7.8	8.5	7.1	**7.8**	4.9	5.3	5.1	**5.1**	5.9	4.3	4.2	**4.8**
14-Dec	Base	5.2	5.4	4.4	**5.0**	3.6	4.2	4.3	**4.0**	4.1	2.7	2.7	**3.2**
21-Dec	Base	6.1	5.4	5.2	**5.6**	2.8	2.3	3.4	**2.8**	3.8	3.5	3.5	**3.6**
4-Feb	Base	5.0	5.5	4.0	**4.8**	1.9	1.5	2.5	**2.0**	2.3	2.7	1.0	**2.0**
23-Nov	Subbase	24.1	23.2	31.9	**26.4**	16.8	16.2	15.2	**16.1**	25.5	16.9	19.4	**20.6**
30-Nov	Subbase	9.8	10.9	9.6	**10.1**	8.3	8.5	8.9	**8.6**	10.9	12.9	10.0	**11.3**
2-Dec	Subbase												
7-Dec	Subbase	10.7	7.8	6.1	**8.2**	8.1	11.1	6.8	**8.6**	6.4	7.3	4.7	**6.1**
14-Dec	Subbase	7.5	8.2	6.6	**7.4**	7.3	7.1	13.3	**9.2**	8.3	6.0	5.4	**6.5**
21-Dec	Subbase	6.4	7.7	6.0	**6.7**	10.6	7.9	10.5	**9.7**	6.7	7.4	4.9	**6.4**
4-Feb	Subbase	4.2	4.9	3.8	**4.3**	8.1	2.0	8.2	**6.1**	3.4	6.4	3.3	**4.3**
23-Nov	Subgrade	22.0	27.0	25.1	**24.7**	28.8	29.6	32.9	**30.5**	25.3	28.5	24.8	**26.2**
30-Nov	Subgrade	16.8	20.5	23.8	**20.4**	25.9	20.8	21.3	**22.7**	23.8	28.7	26.5	**26.3**
7-Dec	Subgrade	16.4	10.2	17.1	**14.6**	24.0	25.0	20.6	**23.2**	13.6	35.0	12.2	**20.3**
14-Dec	Subgrade	16.2	18.3	13.8	**16.1**	24.4	17.8	28.0	**23.4**	20.1	15.5	22.9	**19.5**
21-Dec	Subgrade	17.8	26.8	24.0	**22.9**	45.2	25.6	31.2	**34.0**	17.2	22.4	24.3	**21.3**
4-Feb	Subgrade	5.5	4.9	4.1	**4.8**	29.2	9.4	11.7	**16.8**	8.9	16.8	6.2	**10.6**

Figure 25 shows the average DCP results for subgrade layers of each test section plotted over time. The subgrade layer was not tested prior to subbase treatment since the material would be disturbed by the stabilization equipment. The material was therefore accessed as the lower part of the penetration began at the top of the treated subbase.

As shown in Figure 25, since the embankment soil is untreated and not uniform, the DCP results are fairly scattered among test sections. However, the averaged DCP results also indicate that the overall average stiffness of the untreated subgrade increased from November 2004 (average mm/blow = 28.9) to February 2005 (average mm/blow = 13.6). The increase in subgrade stiffness is likely due to dryer weather conditions that existed during the construction period. In addition, the subsequent layers reduced inundation by shedding any precipitation.

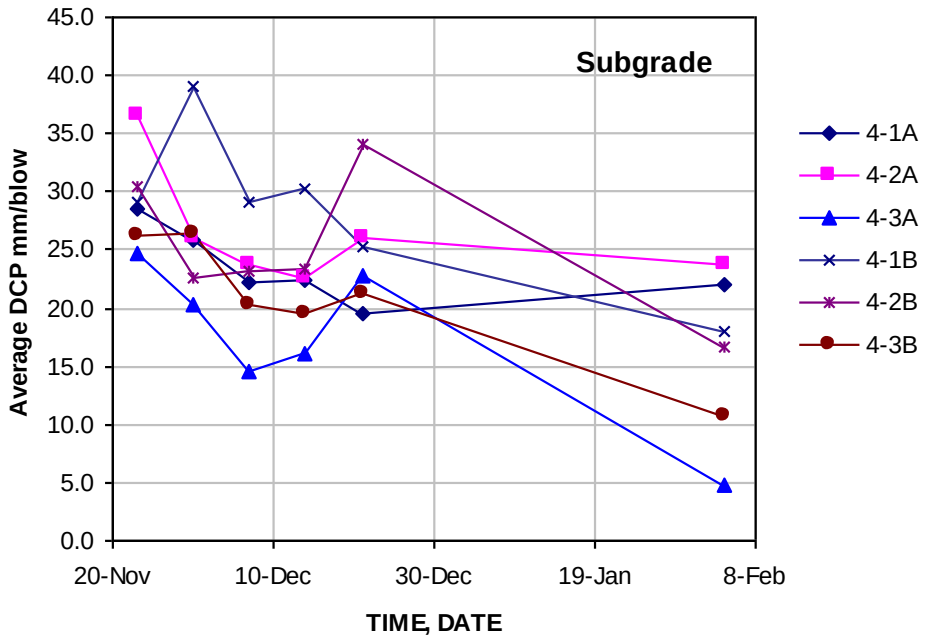

Figure 25
Average DCP results of subgrade layers

Figure 26 provides the average DCP results for subbase layers of each test section plotted over time. Both lime treated and cement treated subbases showed an increase in stiffness over time as indicated by the decreasing DCP results in terms of mm/blow. The DCP results in the lime treated areas (4-1A, 4-1B, and 4-2B) decreased from roughly 31.8 mm/blow to 7.3 mm/blow; whereas, in cement treated areas (4-2B, 4-3A, and 4-3B) the average result went from 20.3 mm/blow to 5.3 mm/blow. In general, the average DCP result for cement treated subbase was found to be smaller than that of a lime-treated subbase, indicating that the cement-treated soils are stiffer than lime-treated soils. Additionally, both treated soils are apparently stiffer than untreated embankment soil as evidenced by smaller DCP values in terms of mm/blow.

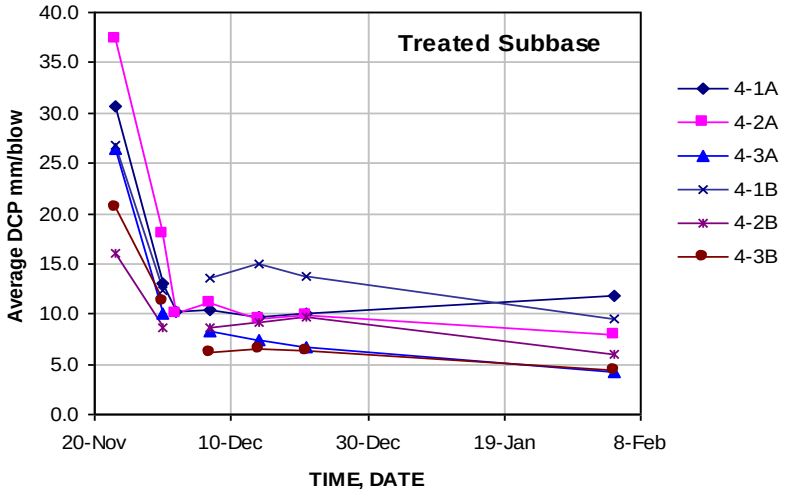

Figure 26
Average DCP results for subbase layers

The average DCP results on various base layers of each test section are plotted in Figure 27. The following observations can be drawn from the DCP results on different base materials as shown in Tables 29-30 and Figure 27:

- All base materials showed a significantly large decrease in the DCP results measured over time, indicating a dramatic stiffness increase after the initial placement.

- The BCS/Slag layer in section 4-1A showed the strongest increase in strength during the course of the DCP testing. The BCS/Flyash layer in section 4-2A also experienced a significant stiffness increase due to the curing effect. Some of the latter tests encountered material so stiff that penetration was not possible (no penetration with 20 blows). This very stiff material was noted as refusal and the hole was extended with a hammer drill to the bottom of this layer so that DCP data for the lower treated subbase and subgrade layers could be collected.

- Raw BCS (First 30 ft. of section 4-2A)

    - DCP results increased in stiffness from 14 mm/blow in November/December to 4.5 mm/blow in February.

- DCP results on the stone section (4-1B and 4-2B) indicated some strength gains due to compaction of the above asphalt surface layer. Initial November/December

average DCP mm/blow was roughly 10 mm/blow. February 2005 results indicated an average of 3 mm/blow.

- DCP results on the two foamed asphalt bases also indicated some strength gains due to compaction of the above asphalt surface layer. Initial November/December average DCP mm/blow was roughly 13.5 mm/blow. February 2005 results indicated an average of 5 mm/blow for section 4-3A and an average of 2 mm/blow for section 4-3B.

- The overall DCP results indicated that the BCS/Slag layer is the strongest base among the seven base materials compared, followed by BCS/Flyash. Also, it appears that the foamed asphalt treated 100 percent RAP base is slightly stronger than the foamed asphalt treated 50 percent RAP and 50 percent recycled soil cement base. Furthermore, the average DCP results of the two foamed asphalt bases are found compatible to the average DCP results obtained on the two stone bases used in sections 4-1B and 4-2B.

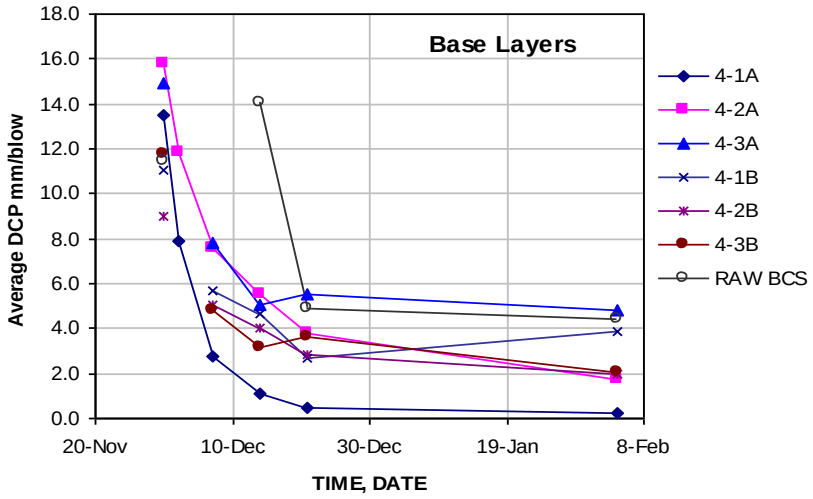

Figure 27
Average DCP results for base layers

FWD Tests. FWD tests were conducted on the top of the completed treated subbase, base, and HMA surface course, beginning shortly after the compaction were completed. The FWD tests were performed at seven stations on each of six sections. The station IDs with the corresponding station numbers are presented in Table 31.

Table 31
FWD test stations

Station ID	ALF Test Sections					
	4-1A	4-1B	4-2A	4-2B	4-3A	4-3B
S1	Sta. 0+41	Sta. 1+48	Sta. 0+41	Sta. 1+48	Sta. 0+41	Sta. 1+48
S2	Sta. 0+45	Sta. 1+52	Sta. 0+45	Sta. 1+52	Sta. 0+45	Sta. 1+52
S3	Sta. 0+49	Sta. 1+56	Sta. 0+49	Sta. 1+56	Sta. 0+49	Sta. 1+56
S4	Sta. 0+53	Sta. 1+60	Sta. 0+53	Sta. 1+60	Sta. 0+53	Sta. 1+60
S5	Sta. 0+57	Sta. 1+64	Sta. 0+57	Sta. 1+64	Sta. 0+57	Sta. 1+64
S6	Sta. 0+61	Sta. 1+68	Sta. 0+61	Sta. 1+68	Sta. 0+61	Sta. 1+68
S7	Sta. 0+65	Sta. 1+72	Sta. 0+65	Sta. 1+72	Sta. 0+65	Sta. 1+72

Figures 28 (a) and 28 (b) present the center FWD deflections measured at two dates on the top of lime-treated and cement-treated subbase courses, respectively. The deflections reported in the figures were measured under the 1,500-lb. FWD load level and normalized to 1,500 lb. The following observations can be made from Figure 28:

- Deflections on both lime-treated and cement-treated subbases decreased over time, indicating that the strengths of both materials increase with the increase curing time.

- Similarly to the DCP results, the cement-treated subbases generally showed smaller center deflections, thus greater in-situ stiffness than the lime-treated subbases.

- Figure 28(a) indicates that the lime-treated subbase on section 4-1A displayed significantly higher center deflections in terms of deflection magnitudes and station variations than those on sections 4-1B and 4-2A. It implies that, in the FWD testing area, the structure strength of the lime-treated subbase course in section 4-1A was possibly weaker than those layers in sections 4-1B and 4-2A. Possible explanations may include: (a) the untreated subbase soil in section 4-2A prior to the addition of the lime seems slightly drier than other lime treatment sections and (b) the PI of the untreated soil on section 4-1B was lower than the other two lime sections.

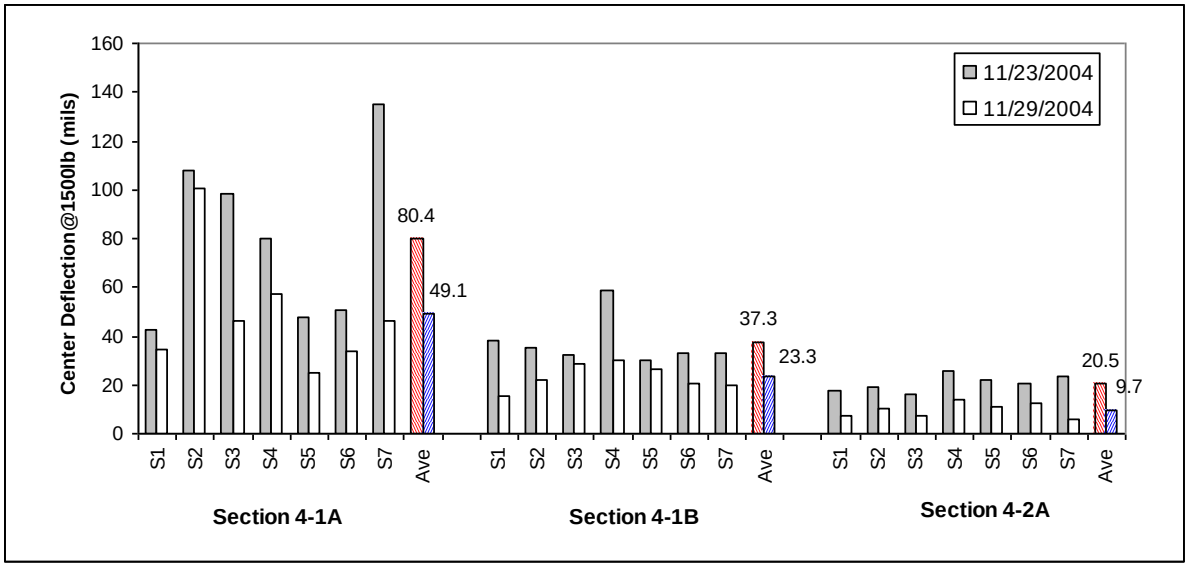

(a) Lime-treated subbase

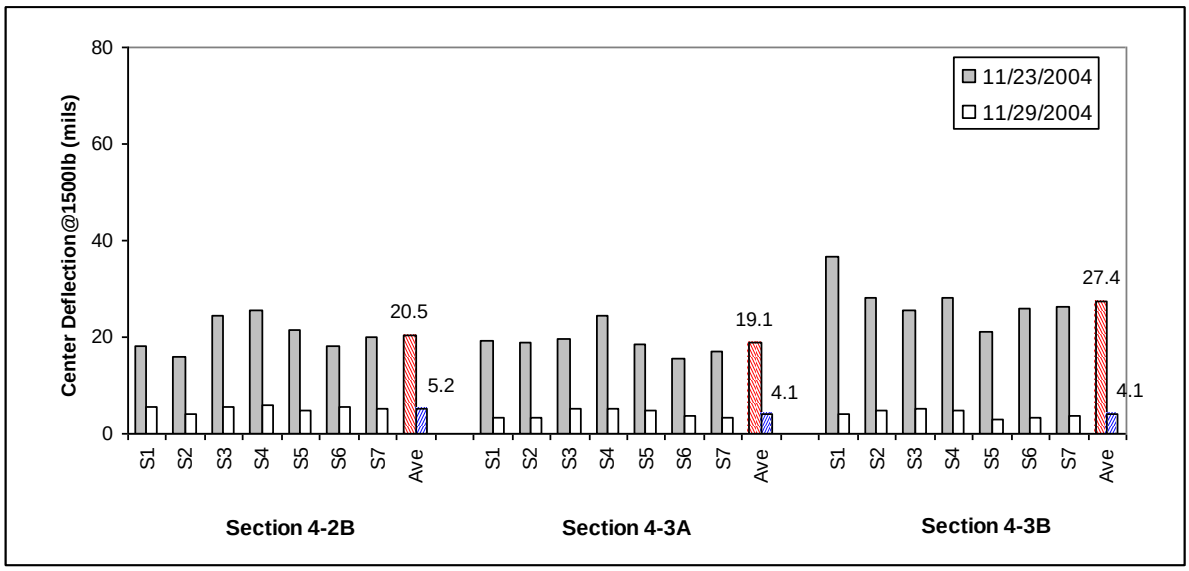

(b) Cement-treated subbase

Figure 28
FWD center deflection on the top of subase layers (1,500 lb.)

- Figure 28(b) shows that the average center deflections on three cement-treated sections 4-2B, 4-3A, and 4-3B were similar, based on the second FWD test results (on Nov. 29, 2004). The deflection variations among stations were also similar in the three cement-treated subbase courses. This indicates that all cement-treated subbase courses possessed comparable structure strengths during the construction. This may

also imply that the effectiveness of the cement treatment on this soil seems less dependent on the construction variation than the lime treatment does.

Figure 29 presents the center FWD deflections measured on the top of base courses at two different dates. The deflections reported in the figure were measured under the 3,000-lb. FWD load level and normalized to 3,000 lb.

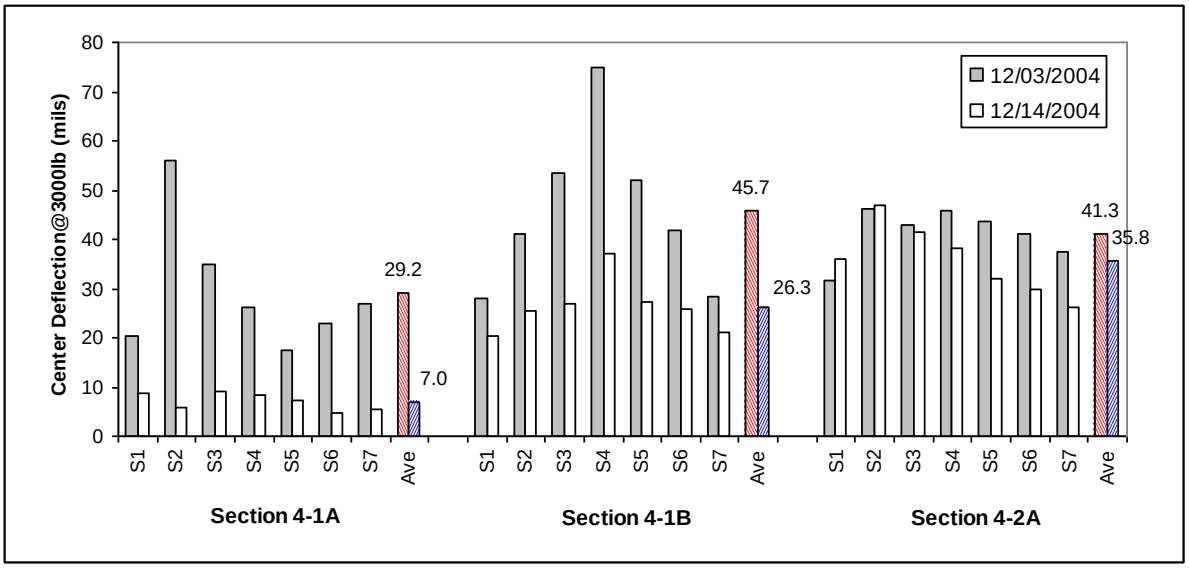

(a) Base courses built over a lime-treated subbase

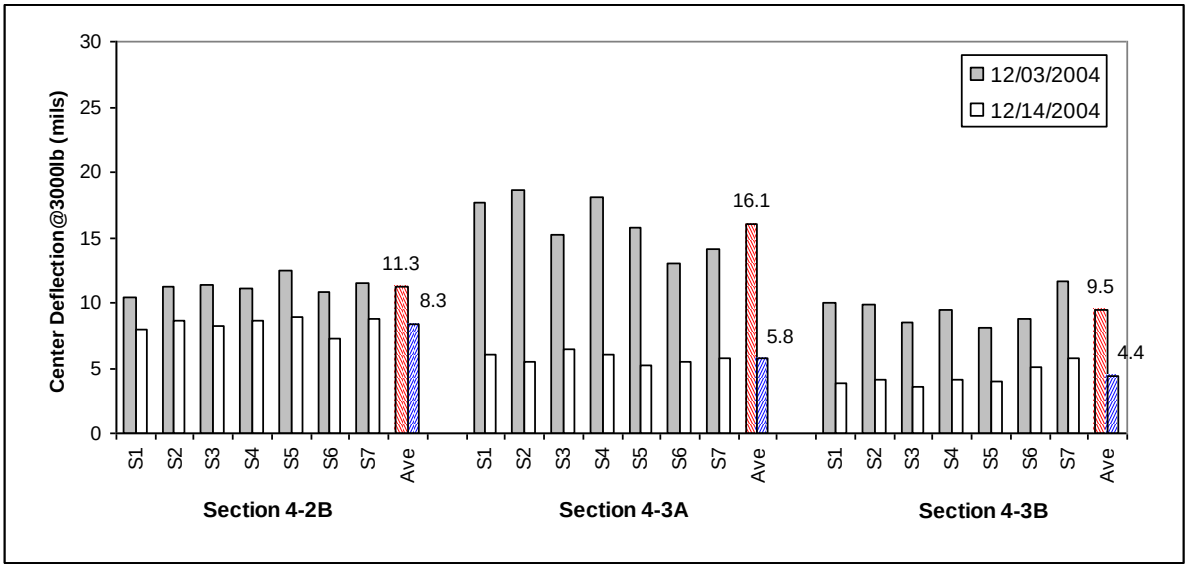

(b) Base courses built over a cement-treated subbase

Figure 29
FWD center deflection on the top of base layers (3,000 lb.)

The following observations can be made from Figure 29:

- Deflections on all test sections generally decreased over time. The reduced deflection indicates an increase in structure strength. The gain in structure strength due to the curing may partially come from beneath the treated soil layers and partially from the base material itself.

- The most significant deflection change was found on the BCS/Slag base of section 4-1A, dropped by 76 percent of its initial value from 29.2 mils to 7.0 mils. This indicates that the stiffness of the BCS/Slag increased significantly after 11 days of curing. Note that such a dramatic stiffness increase was also observed in the DCP results, Figure 27.

- Both foamed asphalt (FA) treated bases were found to have the smallest surface deflections after the curing: 4.4 mils for the FA treated 100 percent RAP and 5.8 mils for the FA treated 50 percent RAP and 50 percent recycled soil cement. However, due to the temperature effect (i.e., it is known that the stiffness of an asphalt mixture can be varied from a very high value at a low temperature to a very low value at a high temperature), the FWD tests conducted on a cooler time of the year (December) may account for those low deflection values.

- By comparing the deflections on sections 4-1B and 4-2B (both with a stone base), it confirmed that the cement-treated subbase should be stronger than the lime-treated subbase.

- The in-situ stiffness of BCS/Flyash appeared to be significantly weaker than BCS/Slag.

- Overall, the BCS/Slag base of section 4-1A showed the highest in-situ stiffness among the group of base materials evaluated.

Figure 30 presents the center FWD deflections measured on the top of HMA layers after the construction. The deflections reported in the figure were measured under the 9,000-lb. FWD load level and normalized to 9,000 lb. In general, the following observations can be drawn from Figure 30:

- The overall structure strength ranking among the six test sections was found to differ slightly when comparing FWD deflections obtained on HMA layers (Figure 30) to

those measured on top of base layers (Figure 29), even though all test sections supposedly have the same HMA thickness of 2 in.

- BCS stabilized with the fly ash was found not as effective as BCS stabilized with the slag, by comparing the deflections on sections 4-1A and 4-2A.

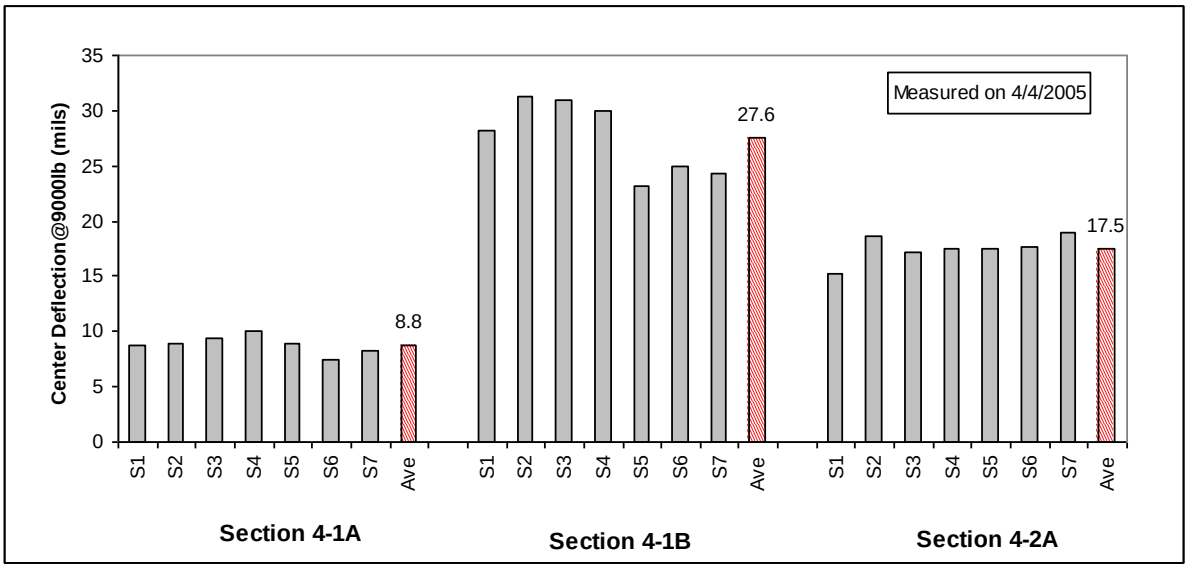

(a)

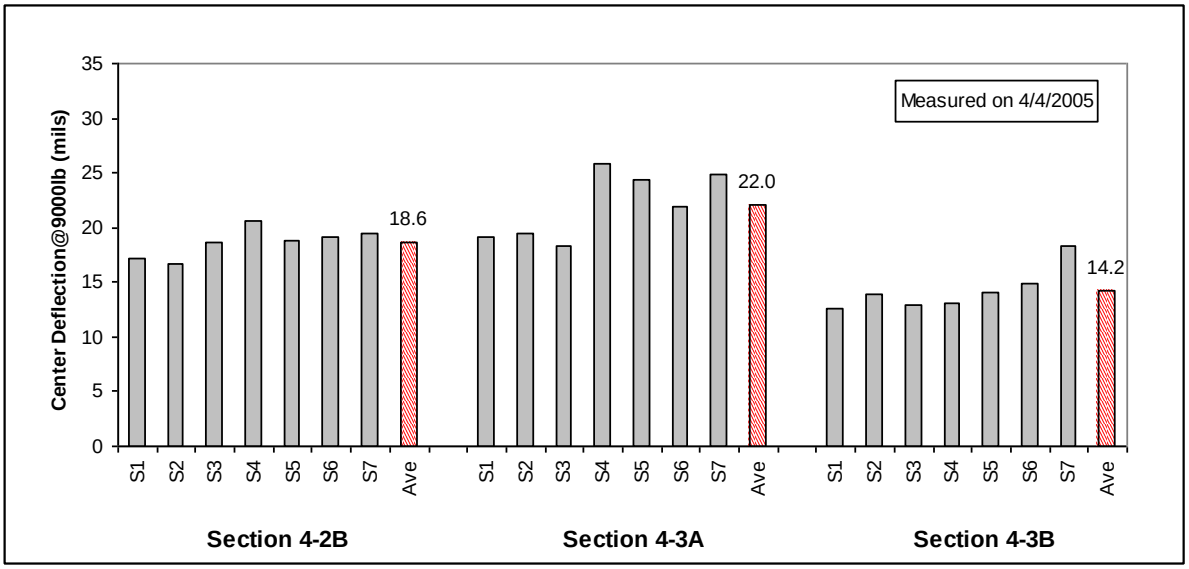

(b)

Figure 30
FWD center deflection on the top of HMA layers (9,000 lb.)

- Both BCS bases seem to be stiffer than a crushed stone base, by comparing the deflections of sections 4-1A and 4-2A to 4-1B.

- The cement-treated subbase was confirmed to be stronger than the lime-treated subbase by comparing the deflections of sections 4-1B and 4-2B.

- FA treated 100 percent RAP base seems to be stiffer than FA treated 50 percent RAP and 50 percent recycled soil cement base (4-3A vs. 4-3B).

- Overall, section 4-1A with BCS/Slag base and lime-treated subbase seems to be the strongest test section in this experiment; whereas, the weakest test section could be section 4-1B, which has a stone base over the lime treated soil layer.

Dynaflect Tests. The Dynaflect tests were performed on April 4, 2005, on the finished HMA layers of each test section immediately after the FWD tests. Figure 31 presents the estimated SN (structural number) and subgrade elastic modulus for the six test sections evaluated. In general, a higher SN value is expected for a pavement structure with a greater load carrying capacity.

The following two observations can be made from Figure 31:

- The SN values generally confirmed the structure strength ranking derived from FWD deflection results (Figures 29 and 30), except for the two foamed asphalt base sections (4-3A and 4-3B). Apparently, temperature effects were found on both FWD and Dynaflect deflection results.

- The subgrade moduli derived from Dynaflect showed similar ranges from 4.3 to 4.8 ksi for all test sections. This is expected since the same embankment soil was used in the construction of all six test sections.

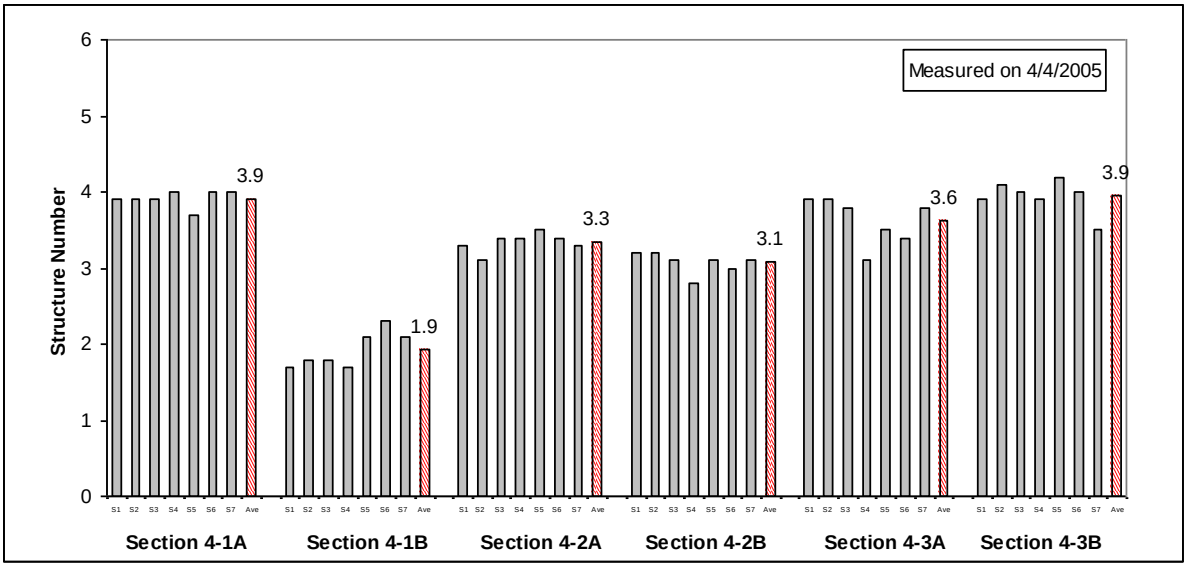

(a) Structure number

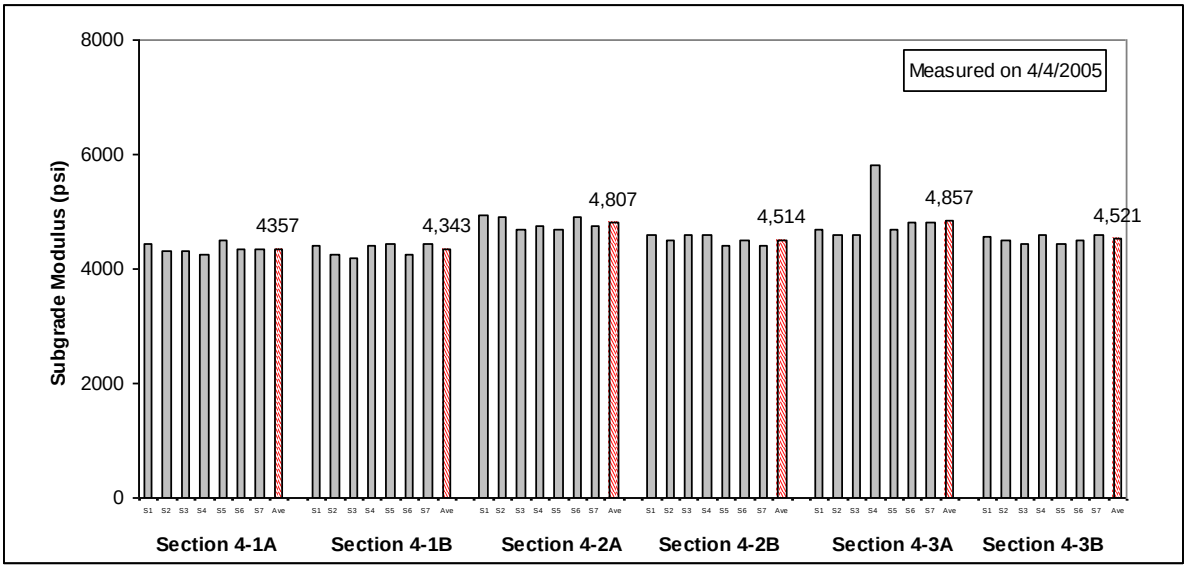

(b) Subgrade modulus

Figure 31
Dynaflect test results

Summary

Six asphalt pavement test sections including four stabilized base materials and two treated subgrade soils were constructed at the LTRC's PRF site. The main purpose of the experiment was to verify and validate the laboratory findings regarding to different base and subbase materials and to provide design parameters for potential field implementation. The test section design was intended to provide an opportunity for direct performance comparison of

various pavement materials using the accelerated pavement testing under southern Louisiana pavement conditions. The direct performance comparison includes: slag stabilized BCS vs. fly ash stabilized BCS, stabilized BCS vs. crushed stone, FA treated 100 percent RAP vs. FA treated with 50 percent RAP and 50 percent recycled soil cement, FA treated materials vs. crushed stone, and lime treated silty clay soil vs. cement treated silty clay soil.

The construction began by removing one existing test lane and shoulder used in a previous experiment. Normal construction practices were followed in accordance with *Louisiana Standard Specifications for Roads and Bridges (2000),* except for the placement of HMA layers in which the paver accepted truck-loaded mixtures directly into its receiving hopper instead of using an MTV (Material Transfer Vehicle) that is required on all paving projects in Louisiana. In general, the construction process went smoothly as planned and the following key as-built measurements were recorded:

- The measured moisture contents for the embankment soil ranged from 18.0 percent to 24.2 percent with an overall average of 20.5 percent, which is about 2 percent higher than the optimum moisture content of 18.5 percent for this soil.

- The average as-built densities on the lime-treated and cement-treated layers were 98.1 percent and 93.1 percent, respectively; the corresponding in-situ average moisture contents were 17.8 percent and 17.9 percent.

- Both stone base layers (in sections 4-1B and 4-2B) received as-built density values greater than 95 percent. However, the four chemically stabilized or treated base materials (BCS/Slag, BCS/Flyash, and two foamed asphalt treated RAP materials) were constructed with lower density values ranging from 80.5 percent to 86.7 percent.

- The as-built air voids of the HMA layers were averaged to 7.2 percent, with a range from 5.5 percent to 9.3 percent among sections. The highest air voids of 9.3 percent was received on section 4-2A, while the lowest air voids of 5.5 percent was on section 4-3B.

- The overall as-built HMA thickness was averaged to be 1.7 in. as compared to the design HMA thickness of 2 in. In addition, the measured thicknesses varied from 1.3 in. to 1.8 in., with the thinnest average HMA thickness of 1.3 in. found in section 4-1B under the ALF loading area, followed by the second thinnest thickness of 1.5 in. in section 4-2B.

During construction, the in-situ instrumentation devices were successfully installed and each pavement section included two pressure cells, one multi-depth deflectometer, and two moisture gages. FWD, Dynaflect, and DCP tests were performed during the construction of individual pavement layers, which can provide valuable information for future pavement performance evaluation. In general, the following common observations were made from the in-situ test results:

- The cement-treated subbase layers displayed significantly higher initial-strengths than the lime-treated subbase layers.
- BCS stabilized with fly ash was found not as effective as BCS stabilized with slag. However, both stabilized BCS bases seem to be stiffer than a crushed stone base.
- FA treated 100 percent RAP bases appeared to be stronger than FA treated 50 percent RAP and 50 percent recycled soil cement bases. However, whether the FA treated bases should be stronger or weaker than the stone base on section 4-2B is unknown.
- Overall, section 4-1A with a BCS/Slag base and lime-treated subbase seemed to be the strongest test section in this experiment; whereas, the weakest test section could be section 4-1B, which has a stone base over the lime treated soil layer.

As a reference, Table 32 presents the breakdown construction costs for each individual section expressed in dollar values. These costs were based on the contract's pricing, which may not necessarily reflect normal contract pricing.

Table 32
Construction costs of each section

Item #	Section 4-1A	Section 4-2A	Section 4-3A	Section 4-1B	Section 4-2B	Section 4-3B
203-06	$ 1,667	$ 1,667	$ 1,667	$ 1,667	$ 1,667	$ 1,667
203-08	500	500	500	500	500	500
302-02				3,589	3,589	
304-05	3,000	3,000		3,000		
502-01	1,010	1,010	1,010	1,010	1,010	1,010
509-01	778	778	778	778	778	778
703-03	948	948	948	948	948	948
727-01	28,333	28,333	28,333	28,333	28,333	28,333
S-003			13,995			13,995
S-004	1,250	1,250	1,250	1,250	1,250	1,250
S-014		1,855				
S-015	4,852					
S-016			2,545		2,545	2,545
Sub-Total	$ 42,338	$ 39,341	$ 51,026	$ 41,075	$ 40,620	$ 51,026